Elsevier Editorial System(tm) for Nuclear Inst. and Methods in Physics Research, A
Manuscript Draft

Manuscript Number: NIMA-D-19-00217R1

Title: Development of an alpha-particle imaging detector based on a low radioactive micro-time-projection chamber

Article Type: Full length article

Section/Category: Space Radiation and Underground Detectors

Keywords: Alpha-particle detector; Position sensitivity; Time projection; chamber; ¥mu$-PIC; Low background

Corresponding Author: Dr. Hiroshi Ito,

Corresponding Author's Institution: ICRR, University of Tokyo

First Author: Hiroshi Ito

Order of Authors: Hiroshi Ito; Takashi Hashimoto; Kentaro Miuchi, Ph. D; Kazuyoshi Kobayashi, Ph. D; Yasuo Takeuchi, Ph. D; Kiseki D Nakamura, Ph. D; Tomonori Ikeda; Hirohisa Ishiura

Abstract: An important issue for rare-event-search experiments, such as the search for dark matter or neutrinoless double beta decay, is to reduce radioactivity of the detector materials and the experimental environment. The selection of materials with low radioactive impurities, such as isotopes of the uranium and thorium chains, requires a precise measurement of surface and bulk radioactivity. Focused on the first one, an alpha-particle detector has been developed based on a gaseous micro-time-projection chamber. A low-$¥alpha$ $¥mu$-PIC with reduced alpha-emission background was installed in the detector. The detector offers the advantage of position sensitivity, which allows the alpha-particle contamination of the sample to be imaged and the background to be measured at the same time. The detector performance was measured by using an alpha-particle source. The measurement with a sample was also demonstrated and the sensitivity is discussed.

Development of an alpha-particle imaging detector based on a low radioactive micro-time-projection chamber

H. Ito[a*], T. Hashimoto[a], K. Miuchi[a], K. Kobayashi[b,c],Y. Takeuchi[a,c], K. D. Nakamura[a],T. Ikeda[a], and H. Ishiura[a]

[a] *Kobe University, Kobe, Hyogo 657-8501, Japan.*

[b] *Institute for Cosmic Ray Research (ICRR), the University of Tokyo, Kashiwa, Chiba 277-8582 Japan.*

[c] *Kavli Institute for the Physics and Mathematics of the Universe (WPI), The University of Tokyo Institutes for Advanced Study, University of Tokyo, Kashiwa, Chiba 277-8583, Japan.*

Abstract

An important issue for rare-event-search experiments, such as the search for dark matter or neutrinoless double beta decay, is to reduce radioactivity of the detector materials and the experimental environment. The selection of materials with low radioactive impurities, such as isotopes of the uranium and thorium chains, requires a precise measurement of surface and bulk radioactivity. Focused on the first one, an alpha-particle detector has been developed based on a gaseous micro-time-projection chamber. A low-α μ-PIC with reduced alpha-emission background was installed in the detector. The detector offers the advantage of position sensitivity, which allows the alpha-particle contamination of the sample to be imaged and the background to be measured at the same time. The detector performance was measured by using an alpha-particle source. The measurement with a sample was also demonstrated and the sensitivity is discussed.

Keywords: Alpha-particle detector, Position sensitivity, Time projection chamber, μ-PIC, Low background

1. Introduction

Approximately 27% of the universe is dominated by non-baryonic matter, called dark matter. Although many experimental groups have been searching for dark matter, any direct detection has yet been detected. Typical experiments that search for dark matter are performed by using massive, low-background detectors. Although the DAMA group has observed the annual modulation of dark matter particles in the galactic halo with a significance of 9.3σ [1], other groups such as XENON1T [2] and LUX [3] did not report compatibles results. Meanwhile, a direction-sensitive method has been focused because of an expected clear anisotropic signal due to the motion of the solar system in the galaxy [4]. The NEWAGE group precedes a three-dimensionally sensitive dark matter search with a micro-time-projection chamber (micro-TPC), being the main background surface alpha particles from ^{238}U and ^{232}Th in the detector materials or in the μ-PIC [5].

Neutrinoless double beta ($0\nu\beta\beta$) decay is a lepton-number-violating process, which suggests the neutrino as a Majorana particle (i.e. it is its own antiparticle). Experiments like GERDA [6] and KamLAND-Zen [7] have been able to set a lower limit on the half-life over 10^{25} yr and 10^{26} yr at 90%CL by using ^{76}Ge and ^{136}Xe, respectively, but no positive signal of the $0\nu\beta\beta$ process has not be observed yet. Conversely, a tracking system for two electrons provides strong evidence of the $0\nu\beta\beta$ decay process. The $0\nu\beta\beta$ background has been well investigated as radioactive impurities such as ^{238}U and ^{232}Th decay-chain isotopes, ^{40}K, ^{60}Co, ^{137}Cs including in the detector material, which emit γ with around MeV [8, 9]. The NEMO3 group set lower limits at

*Corresponding author. E-mail address: ito.hiroshi@crystal.kobe-u.ac.jp (H. Ito).

$T_{1/2}(0\nu\beta\beta) > 2.5 \times 10^{23}$ yr (90%CL) for ^{82}Se [10], and $T_{1/2}(0\nu\beta\beta) > (1.1 - 3.2) \times 10^{21}$ yr (90%CL) for ^{150}Nd [11] for this experiment background is dominated by the ^{208}Tl and ^{214}Bi contamination present in the double beta emitter source foils. The SuperNEMO group has developed the BiPo-3 detector to measure the radioactive impurities in these foils with a sensitivity less than 2 μBq/kg (90%CL) for ^{208}Tl and 140 μBq/kg (90%CL) for ^{214}Bi [12]. Therefore, the background of $0\nu\beta\beta$ decay is not only a contamination by the end point of continuous energy in an ordinary $2\nu\beta\beta$ decay process, but also the radiative impurities such as ^{238}U and ^{232}Th in the detector.

To estimate the radioactive impurities in the detector materials, the XMASS group measured ^{210}Pb and ^{210}Po in the bulk of copper by using a commercial alpha-particle detector (Ultra-Lo 1800, XIA) [13]. The alpha detector has a good energy resolution (as explained in Sec. 3.2) and a mechanism to reduce the background by waveform analysis, and thus a sensitivity is $\sim 10^{-4}$ α/cm^2/hr. However, it has no position sensitivity. A sample such as a micro pattern gas detector board does not have a uniform radioactive contamination. For example the impurities can be in a particular location due to the manufacturing process. Therefore, a position-sensitive alpha detector is required to select materials for the rare-event-search experiments.

This paper is organized as follows. The details of the alpha-particle detector, setup, low-α micro pixel chamber (μ-PIC), gas circulation system, electronics, and trigger data acquisition system are described in Sec. 2. The performance check that uses the alpha-particle source, a sample test, and background estimation are described in Sec. 3. The remaining background of the detector and future prospects are discussed in Sec. 4. Finally, main conclusions are presented in Sec. 5.

2. Alpha-particle imaging detector based on gaseous micro-TPC

A new alpha-particle detector was developed based on a gaseous micro-TPC upgraded from the NEWAGE-0.3a detector [14] which was used to search for dark matter from September, 2008 to January, 2013. The detector consisted of the micro-TPC using a low-α μ-PIC as readout, a gas circulation system, and electronics, as shown in Fig.1. The TPC was enclosed in a stainless-steel vessel for the gas seal during the measurement.

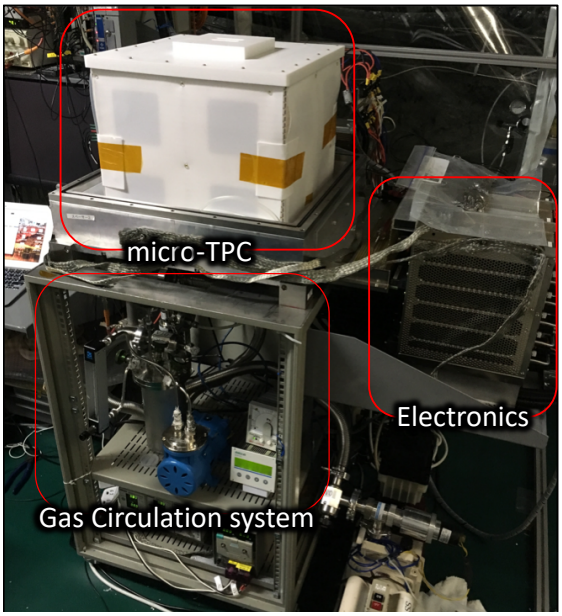

Fig. 1: Photography of the experimental setup. The detector system is composed of a micro-TPC, a gas circulation system, and electronics. The stainless-steel vessel is uncovered so that the outer view of the TPC field cage can be viewed.

2.1. Setup and configuration

Figure 2 shows a schematic view of the detector, where the gas volume is (35 cm $\times$ 35 cm) $\times$ 31 cm. The detector was placed underground at the Kamioka facility in the Institute for Cosmic Ray Research, Japan. An oxygen-free copper plate with a surface electro-polished to a roughness of 0.4 μm and a size of (35 cm $\times$ 35 cm) $\times$ 0.1 cm was used as the drift plate. The drift plate had an opening with a size of 9.5 cm $\times$ 9.5 cm as a sample window. A copper mesh made of 1-mm-ϕ wire in 1-cm pitch (aperture ratio of 0.81) was set on the drift plate to hold the sample at the window area, as shown in Fig. 3. The electrons ionized by the alpha particles drift toward the μ-PIC with a vertical upward-pointing electric field E. CF_4 gas (5N grade: a purity of 99.999% or more), which was also used in the NEWAGE-0.3a, was used as the chamber gas because of the low diffusion properties. The pressure was set at 0.2 bar as a result of the optimization between the expected track length and the detector stability. The track length was expected

to be longer, which improved the tracking performance when the gas pressures were low, while the discharge rate of the μ-PIC increased. The range of 5 MeV alpha particle is $\sim$8 cm in 0.2 bar CF_4 gas, which would provide a reasonable detection efficiency considering the detector size. The electric field in the drift volume, $E = 0.4$ kV/cm/bar, was formed by supplying a negative voltage of 2.5 kV and placing field-shaping patterns with chain resistors every centimeter [15]. The drift velocity was 7.4 ± 0.1 cm/μs. The μ-PIC anode was connected to +550 V. The typical gas gain of μ-PIC was 10^3 at $\sim$ 500 V.

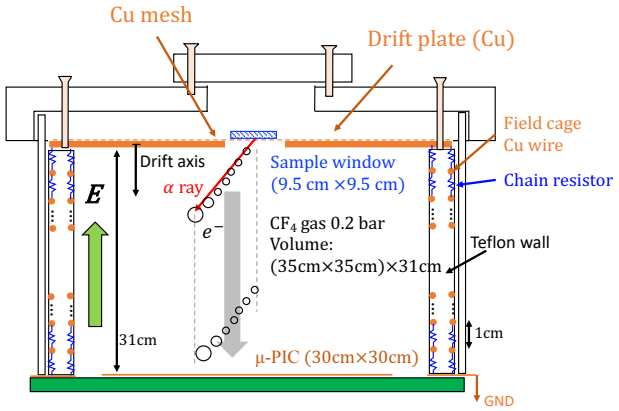

Fig. 2: Schematic cross section of detector setup. Sample window size is 9.5 cm × 9.5 cm. Electric field is formed by a drift plate biased at -2.5 kV and copper wires with 1 cm pitch connecting with chain registers.

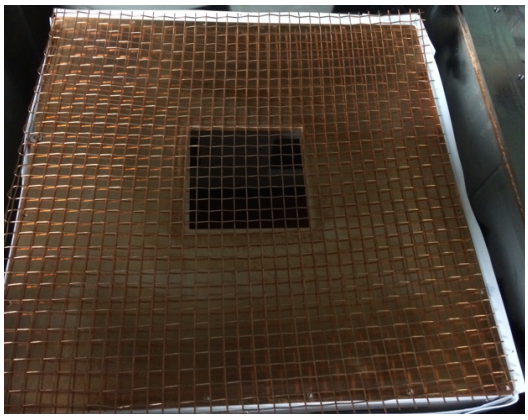

Fig. 3: Drift plate with a sample window (hole size is 9.5 cm × 9.5 cm) and copper support mesh.

2.2. Low-α μ-PIC

The background study for the direction-sensitive dark matter search suggests that μ-PIC has radioactive impurities of ^{238}U and ^{232}Th which emit alpha particles [5]. A survey with a HPGe detector revealed that μ-PIC's glass cloth was the main background source, and so the impurities were removed [16]. Details of the device with the new material, a low-α μ-PIC, will be described in Ref [17].

2.3. Gas circulation system

A gas circulation system that uses activated charcoal pellets (Molsievon, X2M4/6M811) was developed for following purposes: a suppression of radon background and a prevention of gain deterioration due to the outgassing. A pump (EMP, MX-808ST-S) and a needle-type flow-meter (KOFLOC, PK-1250) were used to flow the gas at a rate of $\sim$ 500 cm^3/min. The gas pressure was monitored to ensure the stable operation of the circulation system, operating within $\pm$2% for several weeks.

2.4. Electronics and trigger data acquisition system

The electronics for the μ-PIC readout consisted of amplifier-shaper discriminators [18] for 768 anode and 768 cathode signals and a position-encoding module [19] to reconstruct the hit pattern. A data acquisition system consisted of a memory board to record tracks and a flash analog-to-digital converter (ADC) for the energy measurement. The flash ADC with 100 MHz sampling recorded the sum signal of the cathode strips with a full time range of 12 μs. The anode sum signal issued the trigger. The trigger is occurred when the electrons closest to the detection plane (indicated with the largest circle (e^-) in Fig. 2) reach the μ-PIC. Since the main purpose of the detector is the alpha particle from the sample, the emission position of the alpha particle in the anode-cathode plane was determined at the position most distant from the μ-PIC in the track (the smallest circle in Fig. 2).

3. Performance check

3.1. Alpha-particle source

A 10 cm × 10 cm copper plate with ^{210}Pb accumulated on the surface was used as an alpha-particle source for the energy calibration and energy-resolution measurement [13]. The source emits alpha particles with an energy of 5.3 MeV as a decay of ^{210}Po. The alpha-particle emission

rate (hereinafter called the α rate) of the source plate was calibrated to be 1.49 ± 0.01 α s^{-1} for 4.8–5.8 MeV by using the Ultra-Lo 1800 [13].

3.2. Energy calibration

An energy calibration was conducted with the alpha-particle source (5.3 MeV). The energy was converted from the charge integrated the voltage in time of flash ADC. In this paper, the alpha-particle equivalent is used as the energy unit, MeV. Figure 4 shows a typical energy spectrum of the alpha-particle source. The energy resolution was estimated to be 6.7% (1σ) for 5.3 MeV, which is worse than the Ultra-Lo 1800 resolution of 4.7% (1σ) for 5.3 MeV. This deterioration was thought to be due to the gain variation of the μ-PIC detection area.

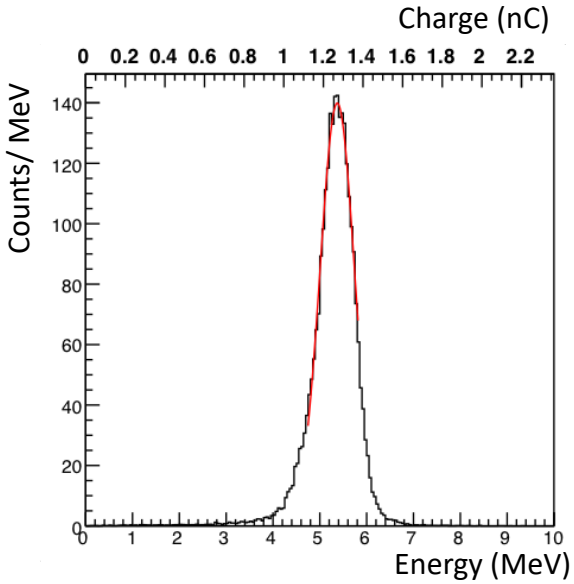

Fig. 4: Energy spectrum for alpha particles from ^{210}Po (5.3 MeV). Red line is a fit result with a Gaussian.

3.3. Event reconstruction

Figure 5 shows a typical event display with the tracks and flash ADC waveform data for alpha-particle emission from ^{210}Po. The hit points were determined based on coincidence of anode and cathode detections. Figure 5 (c) shows the anode-cathode plane for the track. The open circles correspond to hits registered in data. The red solid line is a linear fit result. The dashed line represents the edge of the sample window. The solid blue point is the emission point of the alpha particle. The scheme of the determination of the emission point, or the track sense, is explained in Sec. 3.4. Figure 5 (a) and (d) show anode- and cathode-drift planes, respectively. The drift coordinate is converted from the timing and is set to zero base, which corresponds to the drift-plate position. Figure 5 (b) shows a flash ADC waveform.

The track angles were determined on the anode-cathode, anode-drift, and cathode-drift planes. These angles were determined with a common fitting algorithm. First, the weighted means of the hit points $(x_{\rm w}, y_{\rm w})$ were defined as

$$\begin{pmatrix} x_{\rm w} \\ y_{\rm w} \end{pmatrix} = \frac{1}{n} \sum_{j=0}^{n} \begin{pmatrix} x_j \\ y_j \end{pmatrix}, \quad (1)$$

where x_j and y_j are the measured hit points and n is the number of points. Next, the track was shifted and rotated through the angle θ as follows

$$\begin{pmatrix} x'_j \\ y'_j \end{pmatrix} = \begin{pmatrix} \cos\theta & -\sin\theta \\ \sin\theta & \cos\theta \end{pmatrix} \begin{pmatrix} x_j - x_{\rm w} \\ y_j - y_{\rm w} \end{pmatrix}. \quad (2)$$

Here x'_j and y'_j are the points after the shift, the rotation angle θ were determined to minimize the quantity f, which is defined as

$$f(\theta) = \sum y'^2_j, \quad (3)$$

where this formula means a sum of the square of the distance between the rotated point and the x axis. This method has the advantage to determine the angle with no infinity pole at $\theta = 90°$ (i.e. parallel or perpendicular to the μ-PIC plane) in contrast with a linear fit.

3.4. Track-sense determination

Backgrounds in low radioactivity alpha-particle detectors are in general alpha particles from the radon (radon-α) and material in the detector (detector-α). The radon-α's are expected to be distributed uniformly in the gas volume with isotropic directions. The detector-α's are expected to have position and direction distributions specific to their sources. One of the main sources of the detector-α's is the μ-PIC so the directions of α's coming from this component are mostly upward-oriented. Since the direction of alpha particles from the sample are downward, these detector-α's and half of the radon-α's can be rejected by the cut of upward-direction events.

The deposit energy per unit path length, dE/dx of an alpha particle with an initial energy over a few

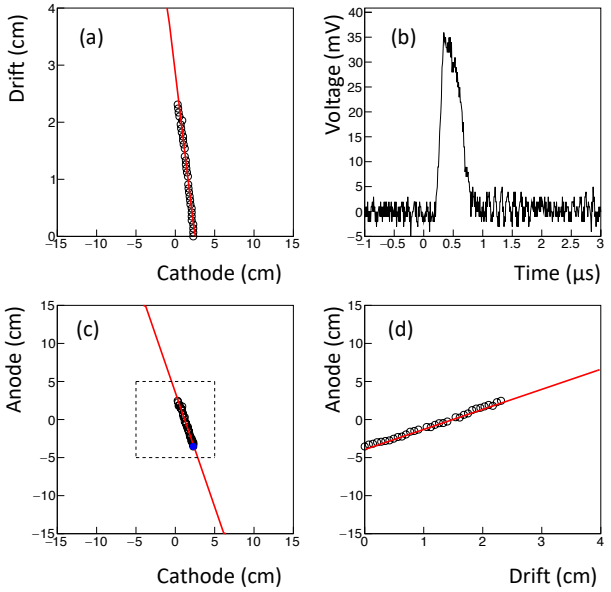

Fig. 5: Event display of an alpha particle from 210Po. (a) cathode-drift projection, (b) flash ADC waveform (c) cathode-anode projection, and (d) anode-drift projection are displayed. The drift coordinate is set to zero base corresponding to the drift plate position for the top of the track.

MeV, has a peak before stopping (Bragg peak). The number of electrons ionized by the alpha particle in the gas is proportional to dE/dx, and dE/dx along the track profile is projected onto the time evolution in the signal due to the mechanism of the TPC. This time profile was recorded as the waveform and thus the track sense (i.e., whether the track was upward or downward) can be determined from the waveform.

A parameter to determine the track sense is

$$F_{\rm dwn} = S_2/(S_1 + S_2), \tag{4}$$

where S_1 and S_2 are the time-integrated waveform before and after the peak. They are defined as

$$S_1 = \int_{t_0}^{t_p} v(t)dt, \tag{5}$$

$$S_2 = \int_{t_p}^{t_1} v(t)dt. \tag{6}$$

Here, $t_0 = 0$ μs, $t_1 = 1.5$ μs, and t_p are the start, stop, and peak time, respectively, for the waveform shown in Fig. 5 (b). The t_p is determined as a time when the voltage is the highest in region between t_0 and t_1. Figure 6 (a) shows typical $F_{\rm dwn}$ distribution with the alpha-particle source, where most of the events are expected to be downward-oriented. The $F_{\rm dwn}$ values of the downward events are distributed around 0.7, as shown by the black-shaded histograms. Conversely, radon-α's have an isotropic direction, i.e., $F_{\rm dwn}$ has two components of upward- and downward-oriented, as shown by the red solid histogram, where the radon-α are background events in the sample test data, as explained later. The scale of the source-α was normalized to the radon-α peak of downward for clarity. Figure 6 (b) shows the efficiency related on $F_{\rm dwn}$ threshold for downward-(black solid) and upward-oriented (blue dashed). The selection efficiency of $F_{\rm dwn} > 0.5$ was estimated to be 0.964 ± 0.004 in the source-α spectrum while the radon background was reduced to half. The blue dashed histogram is a spectrum that subtracted the normalized source-α from the radon-α. The cut efficiency of the upward-oriented events ($F_{\rm dwn} \leq 0.5$) was estimated to be 0.85 ± 0.04. The energy dependence of $F_{\rm dwn}$ will be explained in Sec. 3.6.

3.5. Distribution of emission position

Since alpha particles are mainly emitted from the source, the top points of the alpha-particle tracks trace the shape of the radioactivity on the sample. Figures 7 (a) and 7 (b) show the anode–cathode projection distribution of the top and bottom of the alpha-particle tracks, respectively, where the top and bottom are defined as the zero and maximum drift coordinate, respectively, as shown in Fig. 5 (a) and 5 (d). The dashed line represents the edge of the drift-plate sample window. Comparing Fig. 7 (a) with Fig. 7 (b) clearly reveals the shape of the radioactivity.

The position resolution was evaluated along the four dashed lines in Fig. 7 (a). The number of events was projected onto the axis perpendicular to the lines and was fit with error functions as shown in Fig. 8. Figure 8 (a) and (b) represent the alpha-particle emission position projection to cathode and anode, respectively. The red lines are the fitting based on the error functions. As a result, the position resolution was determined to be 0.68 ± 0.14 cm (σ), where the error is a standard deviation in the four positions.

3.6. Detection and selection efficiency

To select good events for alpha particles from the sample, we use the following criteria: (C1) selection for events with good fitting tracks, (C2) cut

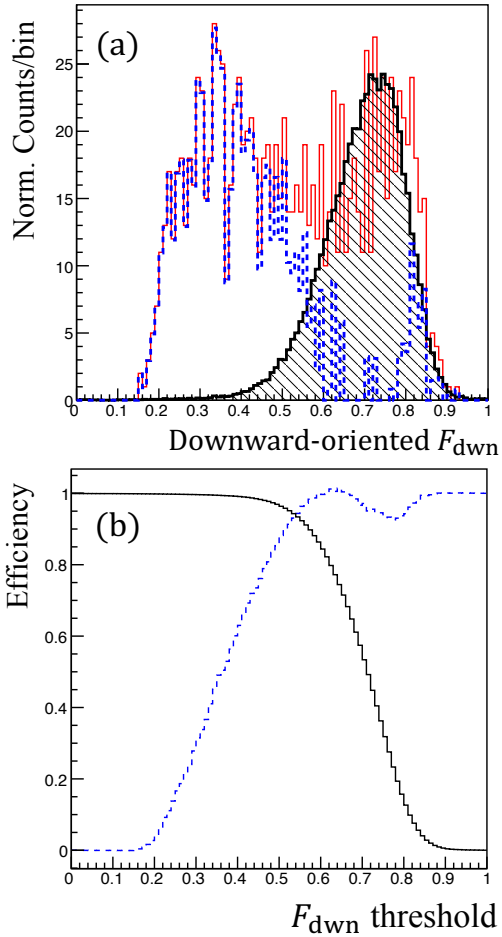

Fig. 6: (a) Downward-oriented distribution for source-α (black shade), radon-α (red solid), and a histogram made by subtracting the radon-α spectrum from the source-α one(blue dashed) (b) Efficiency of downward-(black solid) and upward-oriented (blue dashed) events as a function of F_{dwn} threshold.

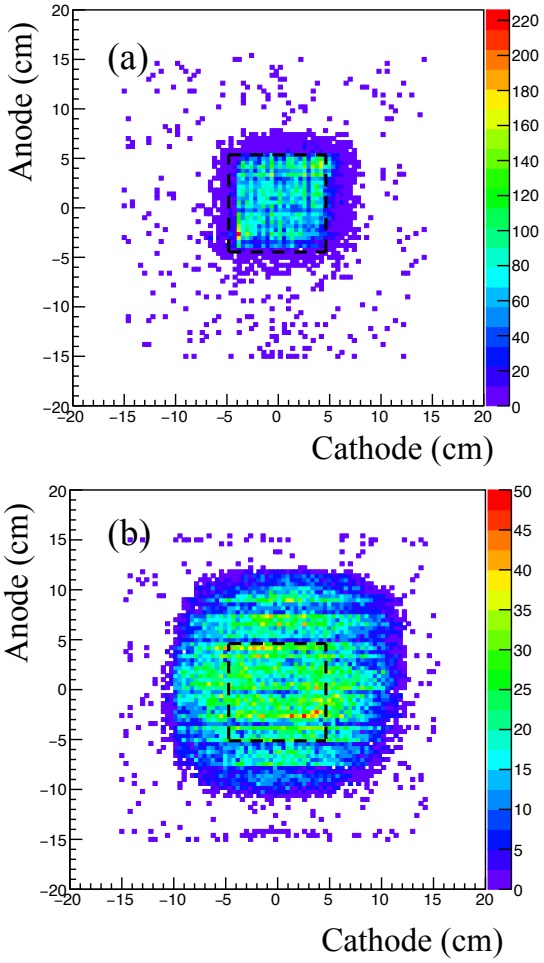

Fig. 7: Anode–cathode projection distributions of (a) top and (b) bottom of tracks for alpha particles emitted from the source. The dashed line is the edge of the sample window.

for the upward-oriented events, and (C3) selection for events with emission points in the sample region.

For criterion C1, the good fit to track events was selected as $f_{\mathrm{min}}(\theta)/(n-1) < 0.02$ cm^2 for the anode-cathode, anode-drift, and cathode-drift planes to remove events that had any noise and to remove candidates for electron tracks, where $f_{\mathrm{min}}(\theta)$ is a minimum of Eq. (3).

Criterion C2 rejects the upward-oriented tracks with > 3.5 MeV and $F_{\mathrm{dwn}} \leq 0.5$ because the determination efficiency depends on the energy. The upward- and downward-oriented tracks can be determined with 95% or more certainly at over 3.5 MeV. Note that this cut was applied for the events > 3.5 MeV, because the radon background, which was assumed to be the dominant background source, created the peak around 6 MeV and the contribution to the energy range below 3.5 MeV was limited.

For criterion C3, the source-α was selected within a region of ± 8 cm in both the anode and cathode, as shown in Fig. 7 (a). The radon-α rate in the selected region was less than a few hundred time of source-α, considering it negligible.

The selection efficiency for C1, C2, and C3 containing the detection efficiency was calculated to be $(2.17 \pm 0.29) \times 10^{-1}$ counts/α (the ratio of the count rate to the α rate of the source), where the error represents the systematic error of C1 to C3 selections and uncertainty of the source radioactivity, being the statistical error negligible.

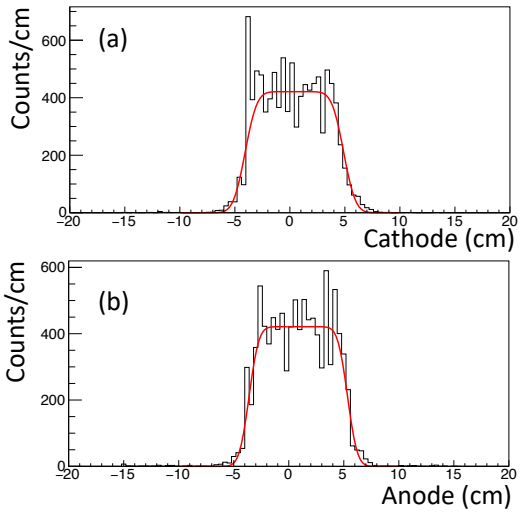

Fig. 8: Alpha-particle emission position projected to cathode (a) and anode (b). Red lines represent fitting with error functions.

3.7. Sample test and background estimate

3.7.1. Setup

A 5 cm × 5 cm piece of the standard μ-PIC whose α rate was known to be 0.28 ± 0.12 α/cm^2/hr in previous work [16] served as a sample and was inspected by using the detector. A photograph of the sample position over the setup mesh is shown in Fig. 9. The measurement live time was 75.85 hr.

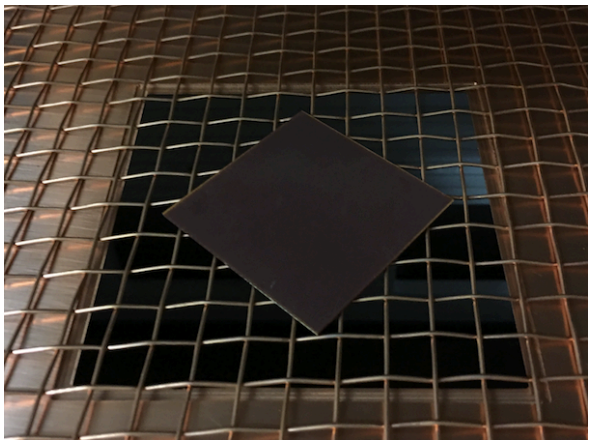

Fig. 9: Setup for a 5 cm × 5 cm piece of the standard μ-PIC as sample.

3.7.2. Background in sample region

The α rate of the sample was estimated by subtracting the background rate. Considered background was mainly the radon-α. The detector measured both the α rates in the region of the sample and around the sample (outer region). The background rate could be determined from the α rate in the outer region. Typically, the upward and downward radon-α rates are same. The sample-α has mainly downward-oriented. Thus, the background rate could be estimated by the upward rate in the sample region and independently cross-checked by the upward rate in the outer region.

We checked the upward-oriented ($F_{\mathrm{dwn}} \leq 0.5$) α rate in both regions because the alpha particles from a sample are typically emitted downward. Measured energy spectra are shown in Fig. 10. The red- and black-shaded histograms show the energy spectra inside and outside the sample region, respectively. These spectra are scaled by the selection efficiency. Both peaks are around 6 MeV and α rates are $(2.16^{+0.54}_{-0.35}) \times 10^{-2}$ (inside) and $(1.54^{+0.64}_{-0.40}) \times 10^{-2}$ α/cm^2/hr (outside). Therefore, the background condition inside the sample region is compatible at less than 1σ with the background condition outside the sample region. The alpha-particle energy spectrum is interpreted as the radon peaks at 5.5 MeV (^{222}Rn), 6.0 MeV (^{218}Po), and 7.7 MeV (^{214}Po).

The downward-oriented ($F_{\mathrm{dwn}} > 0.5$) α rate outside the sample is $(1.58^{+0.29}_{-0.26}) \times 10^{-2}$ α/cm^2/hr, as shown in the black-shaded spectrum of Fig. 11. In this work, the background rate was improved by one order of magnitude in comparison with that of our previous work [16]. The background reduction is attributed to the track-sense determination to reject upward-oriented alpha (for > 3.5 MeV) and the replacement of the low-α μ-PIC (for ≤ 3.5 MeV). In the energy region between 2.0 and 4.0 MeV, where most radon background is suppressed, the background rate is $(9.6^{+7.9}_{-5.6}) \times 10^{-4}$ α/cm^2/hr.

3.7.3. α rate of sample

Figure 12 shows the distribution of the top of the tracks for the sample, where the candidates are selected by the criteria C1 and C2. The regions ① and ② are defined as sample and background regions, respectively. The sample region corresponds to the sample window. The sample region is the inside of ±5 cm of anode and cathode. The background region is the outside of the sample region and the inside of ±7.5 cm of anode and cathode. Figure 11 shows the energy spectra of downward-oriented alpha particles in the sample (red) and the background region (black shaded).

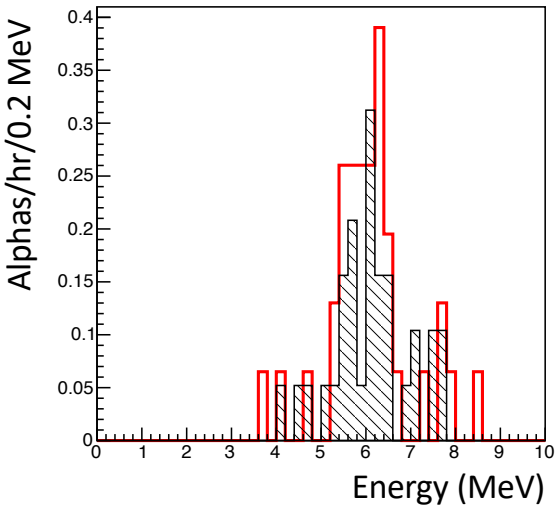

Fig. 10: Upward-oriented alpha-particle energy spectra inside (red) and outside (black shade) the sample region.

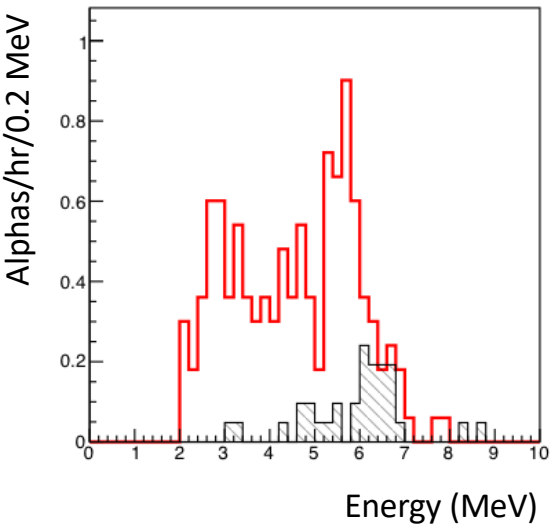

Fig. 11: Downward-oriented alpha-particle energy spectra in sample region (red) and background region (black shade).

The α rate of the sample was calculated to be $(3.57^{+0.35}_{-0.33}) \times 10^{-1}$ α/cm^2/hr ($>$ 2.0 MeV) by subtracting the background rate.

Here, the impurity of ^{232}Th and ^{238}U is estimated by comparing with a prediction of α rate spectrum in the simulation, where it mentions that the isotope in the material is assumed as only ^{232}Th or ^{238}U because of the continuous α rate spectrum. In the fit region between 2 and 10 MeV, the impurity of ^{232}Th or ^{238}U is estimated to be 6.0 ± 1.4 or 3.0 ± 0.7 ppm, respectively. The impurities of ^{232}Th and ^{238}U are measured to be 5.84 ± 0.03 and 2.31 ± 0.02 ppm, respectively, by using the HPGe detector with the measuring time of 308 hr. Although the error is huge because of the continuous energy spectrum, it is consistent with the prediction of prior measurement. In this sample test, it was demonstrated to observe the background alphas at the same time.

4. Discussion

We begin by discussing the sensitivity for the energy between 2 and 9 MeV based on long-term measurements. In this energy range, the background is dominated by the radon-α's with $\sim (1.58^{+0.29}_{-0.26}) \times 10^{-2}$ α/cm^2/hr. The statistical error (σ) is expected to scale with the inverse of the square root of the measurement time (t) given as $\sigma \propto 1/\sqrt{t}$. In this work, the live time was only three days, and the statistical error was $\sigma \sim 3 \times 10^{-3} \alpha$/cm^2/hr. With a measurement time of one month, the error of sample-α's was estimated to be $\sigma \sim 1 \times 10^{-3}$ α/cm^2/hr. When the α rate ($\sigma \sim 1 \times 10^{-3}$ α/cm^2/hr) as the same of the radon-α's ($\sigma \sim 1 \times 10^{-3}$ α/cm^2/hr) was observed, the sum of squares of these σs for the sample and radon-α's would be expected to be a few 10^{-3} α/cm^2/hr as the measurement limit by subtraction with these α rates.

The edges region (anode $\sim \pm 15$ cm or cathode $\sim \pm 15$ cm) has a high rate of background, as shown in Fig. 12. These events have an energy and path-length dependence similar to that of the alpha particles. The alpha particles were mainly oriented upward and were emitted from outside the detection area, limited by the μ-PIC. As an impurity candidate, a piece of the printed circuit board (PCB) was inspected and the α rate was $(1.16 \pm 0.06) \times 10^{-1}$ α/cm^2/hr. Although the alpha-particle events could be rejected by the fiducial region cut, these impurities could be the radon sources (see Fig. 13). Therefore, as a next improvement, a material with less radiative impurities should be used for the PCB.

The goal for detector sensitivity is less than 10^{-4} α/cm^2/hr, which corresponds to measuring radioactive impurities at the ppb level. Here, this level was estimated as an assumption of ^{238}U or ^{232}Th in 1-mm-thick copper plate. We can potentially improve the background rate by using the cooled charcoal to suppress radon gas and using a

	This work	HPGe detector
Sample volume (cm)	$(5 \times 5) \times 0.098$	$(5 \times 5) \times 2.47$
Sample weight (g)	6.8	169.5
Measureing time (hr)	75.85	308
Net α rate (α/cm^2/hr))	$(3.57^{+0.35}_{-0.33}) \times 10^{-1}$	—
^{232}Th impurities (ppm)	6.0 ± 1.4	5.84 ± 0.03
^{238}U impurities (ppm)	3.0 ± 0.7	2.31 ± 0.02

Table 1: Comparison of Screening result with this work and HPGe detector.

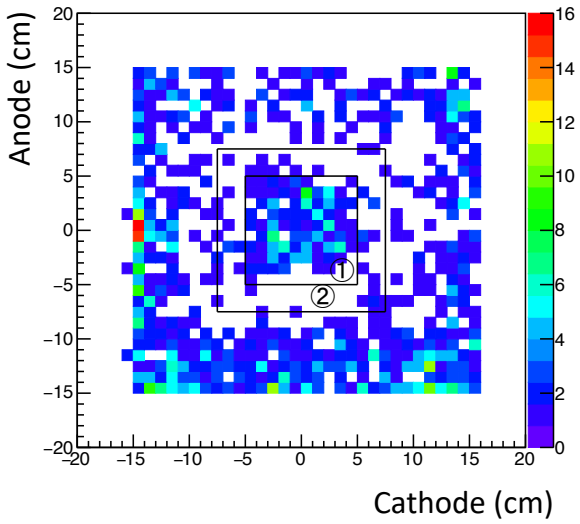

Fig. 12: Distribution of the top of downward-oriented alpha-particle track. The regions ① and ② are the sample and background regions, respectively.

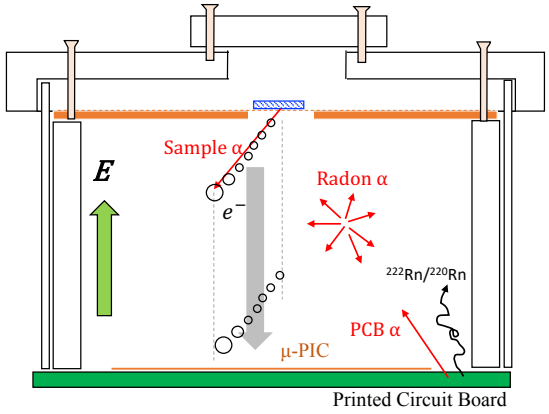

Fig. 13: Schematic cross section of background alpha particles in detector setup.

material with less impurities such as polytetrafluoroethylene, polyimide, and polyetheretherketone without glass fibers. A recent study reported that a cooled charcoal could suppress the radon by 99% in the argon gas [20]. A recent NEWAGE detector suppresses the radon to 1/50 by using cooled charcoal [5]. With these improvements, the detector would achieve to the goal of performance.

5. Conclusion

We developed a new alpha-particle imaging detector based on the gaseous micro-TPC. The measured energy resolution is 6.7% (σ) for 5.3 MeV alpha particles. The measured position resolution is 0.68 ± 0.14 cm. Based on a waveform analysis, the downward-oriented events' selection efficiency is 0.964 ± 0.004 and the cut efficiency of the upward-oriented events is 0.85 ± 0.04 at > 3.5 MeV. Also, a piece of the standard μ-PIC was measured as a sample, and the result is consistent with the one obtained by a measurement done with a HPGe detector. A measurement of the alpha particles from a sample and background was also established at the same time. A background rate near the radon-α ($(1.58^{+0.51}_{-0.42}) \times 10^{-2}$ α/cm^2/hr) was achieved.

Acknowledgments

This work was supported by a Grant-in-Aid for Scientific Research on Innovative Areas, 26104004 and 26104008, from the Japan Society for the Promotion of Science in Japan. This work was supported by the joint research program of the Institute for Cosmic Ray Research (ICRR), the University of Tokyo. We thank Dr. Y. Nakano of the ICRR, University of Tokyo, Japan for providing us with a helium-gas leak detector.

References

[1] R Bernabei, et al., J. Phys. Conf. Ser. **1056** (2018) 012005.
[2] XENON Collaboration, Eur. Phys. J. **77** 881 (2017).

[3] D. S. Akerib, et al., Phys. Rev. Lett. **118** 021303 (2017).
[4] T. Tanimori, et al., Phys. Lett. B **578** (2004) 241.
[5] K. Nakamura, et al., Prog. Theo. Exp. Phys. (2015) 043F01.
[6] The GERDA Collaboration, Nature **544** (2017) 47.
[7] A. Gando, et al., Phys. Rev. Lett. **117** 082503 (2016).
[8] D. S. Leonard, et al., Nucl. Instr. Meth. A **871** (2017) 169.
[9] N. Abgrall, et al., Nucl. Instr. Meth. A **828** (2016) 22.
[10] R. Arnold, et al., Eur. Phys. J. C **78** (2018) 821.
[11] R. Arnold, et al., PRL **119**, 041801 (2017).
[12] A. S. Barabash, et al., JINST **12** (2017) P06002.
[13] K. Abe, et al., Nucl. Instr. Meth. A **884** (2018) 157.
[14] K. Miuchi, et al., Phys. Lett. B **686** (2010).
[15] K. Miuchi, et al., Phys. Lett. B **654** (2007) 58.
[16] T. Hashimoto, et al., AIP Conf. Proc. **1921**, 070001 (2018).
[17] T. Hashimoto, et al., in preparation.
[18] R. Orito, et al., IEEE Trans. Nucl. Scie. **51**, 4 (2004) 1337.
[19] H. Kubo, et al., Nucl. Instr. Meth. A **513** (2003) 93.
[20] M. Ikeda, et al., Radioisotopes, **59**, (2010) 29.

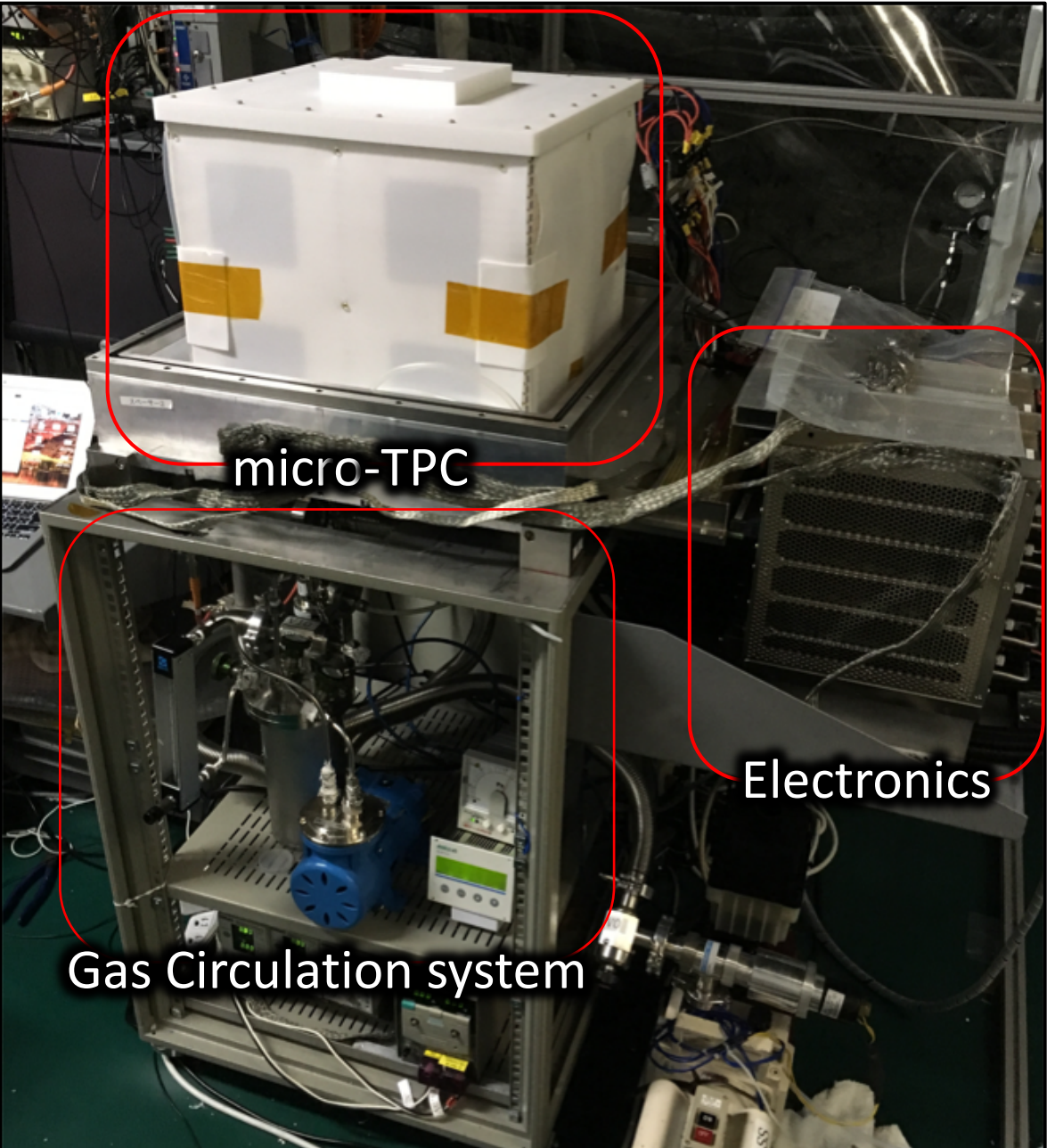
micro-TPC
Electronics
Gas Circulation system

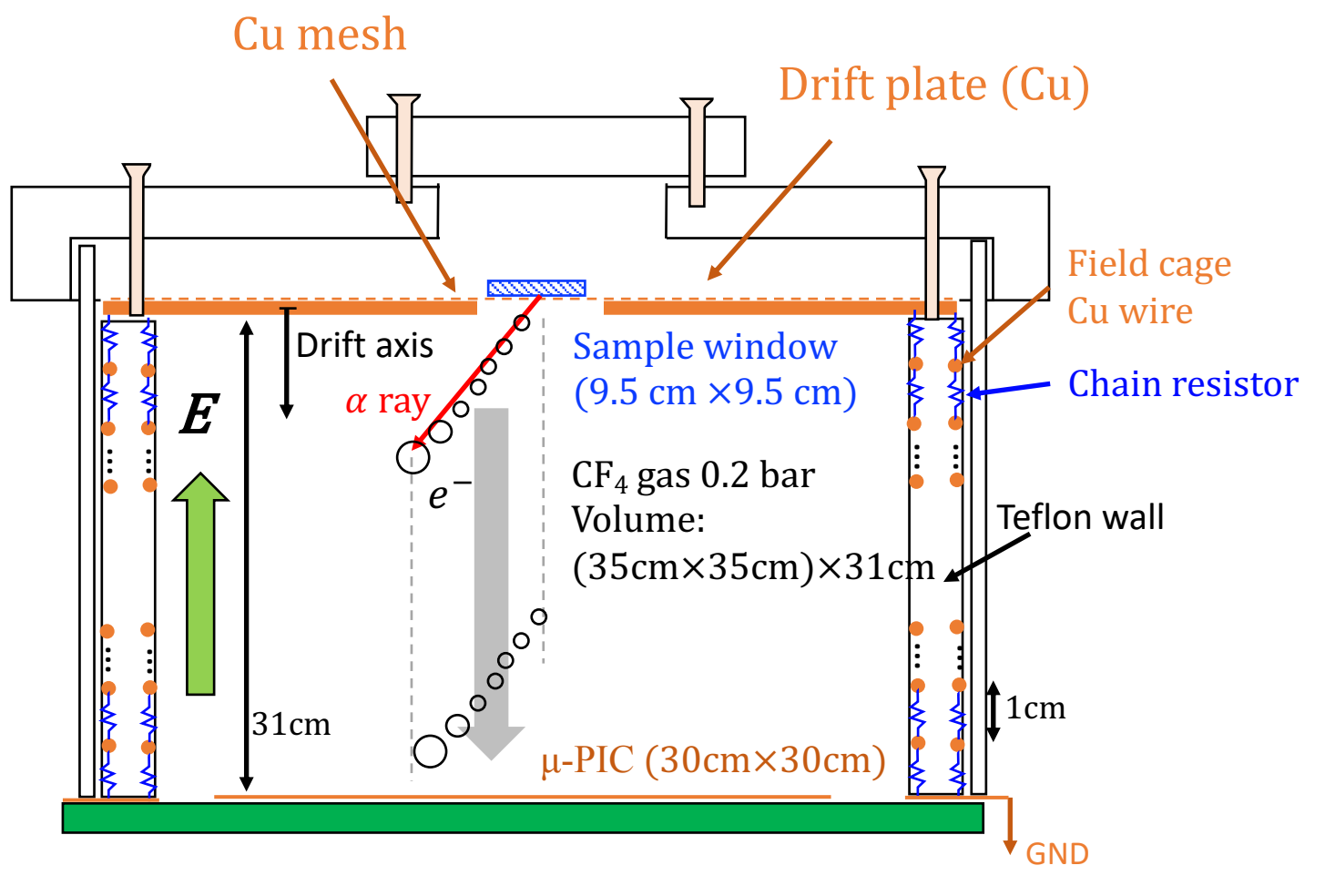
Cu mesh
Drift plate (Cu)
Field cage
Cu wire
Chain resistor
Drift axis
E
α ray
e⁻
Sample window
(9.5 cm ×9.5 cm)
CF4 gas 0.2 bar
Volume:
(35cm×35cm)×31cm
Teflon wall
31cm
1cm
μ-PIC (30cm×30cm)
GND

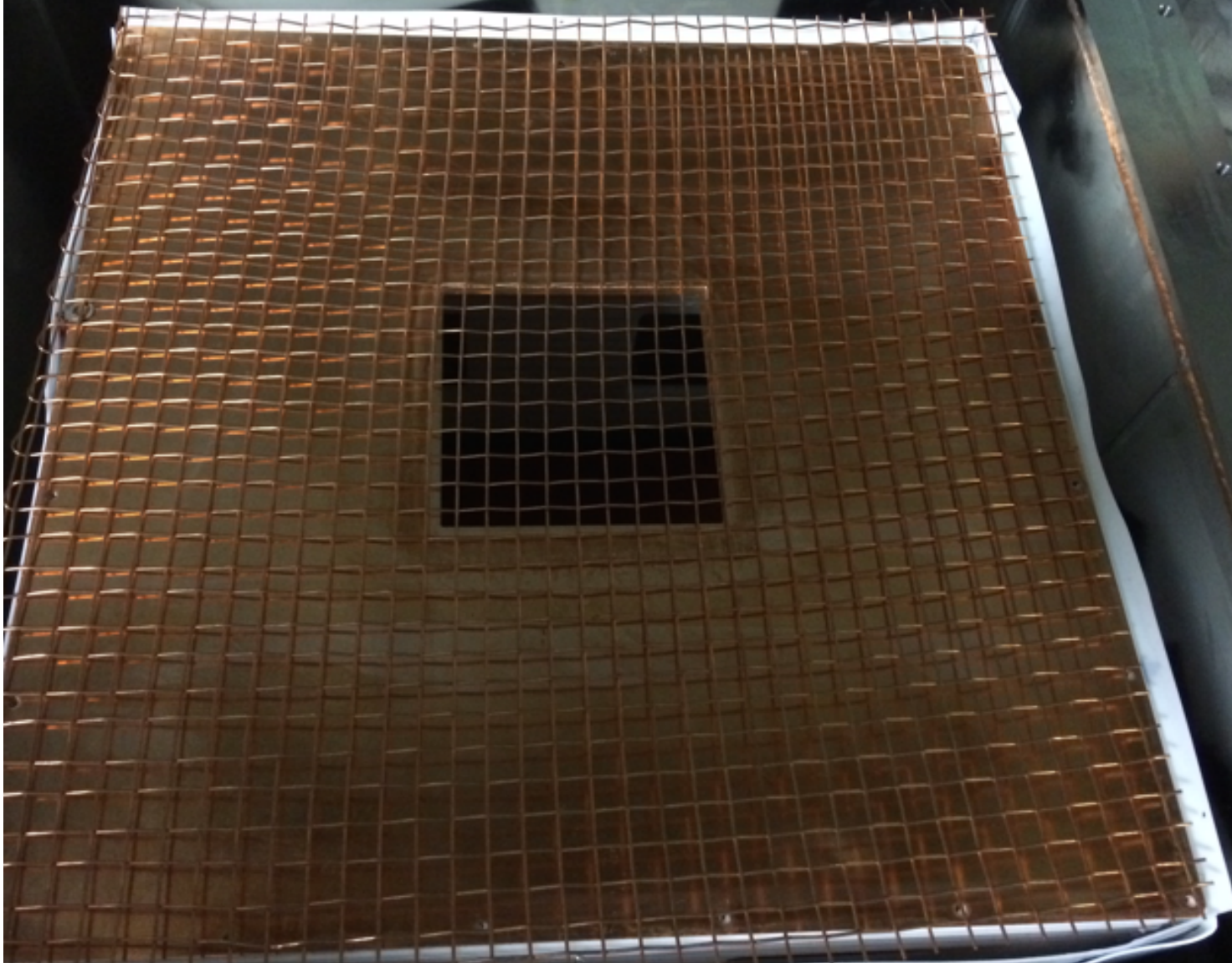

ure4

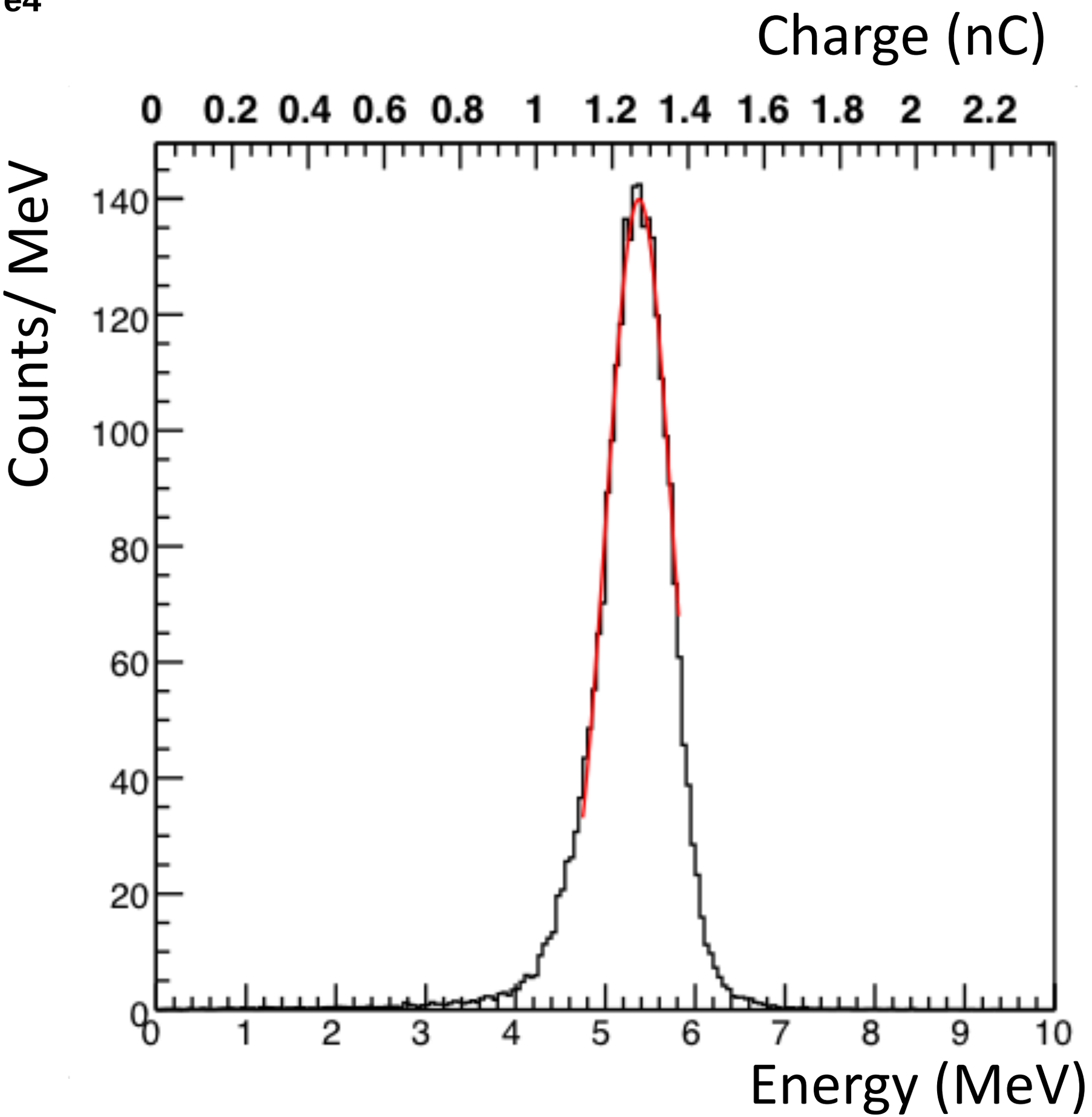
Charge (nC)
0 0.2 0.4 0.6 0.8 1 1.2 1.4 1.6 1.8 2 2.2
Counts/ MeV
140
120
100
80
60
40
20
0
0 1 2 3 4 5 6 7 8 9 10
Energy (MeV)

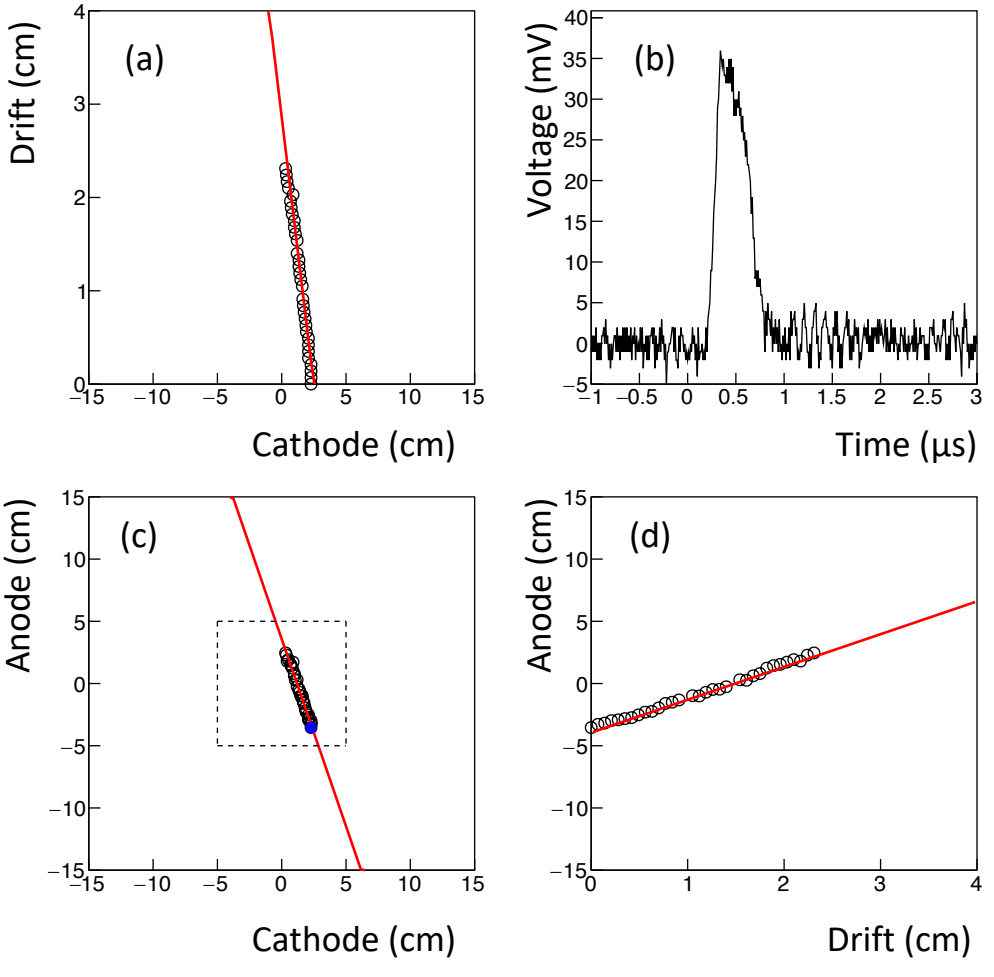
(a)
Drift (cm)
Cathode (cm)
(b)
Voltage (mV)
Time (μs)
(c)
Anode (cm)
Cathode (cm)
(d)
Anode (cm)
Drift (cm)

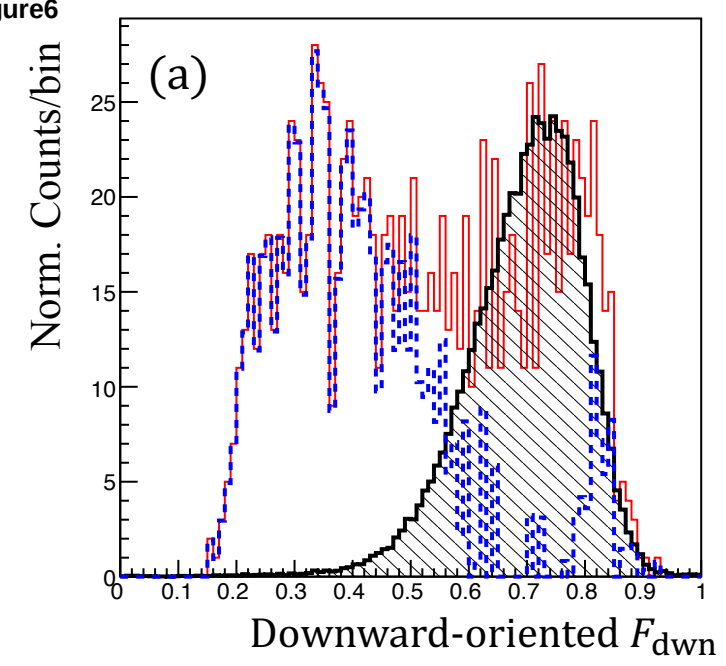
(a)
Norm. Counts/bin
0
5
10
15
20
25
0
0.1
0.2
0.3
0.4
0.5
0.6
0.7
0.8
0.9
1
Downward-oriented F_{dwn}

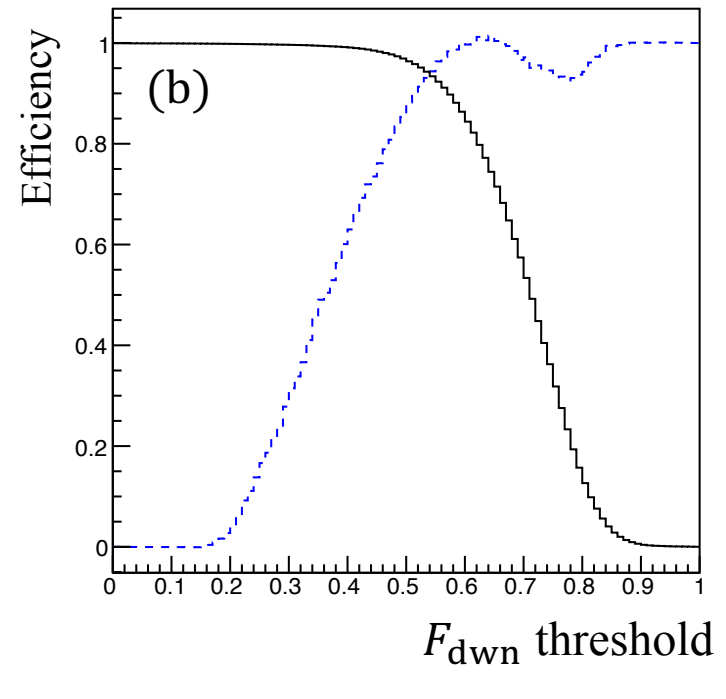
(b)
Efficiency
0
0.2
0.4
0.6
0.8
1
0
0.1
0.2
0.3
0.4
0.5
0.6
0.7
0.8
0.9
1
F_{dwn} threshold

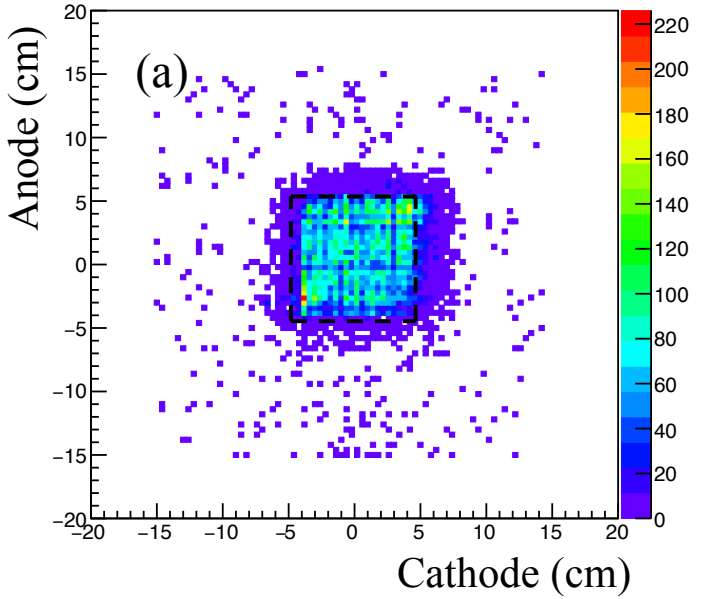
(a)
Anode (cm)
Cathode (cm)
20
15
10
5
0
−5
−10
−15
−20
220
200
180
160
140
120
100
80
60
40
20
0

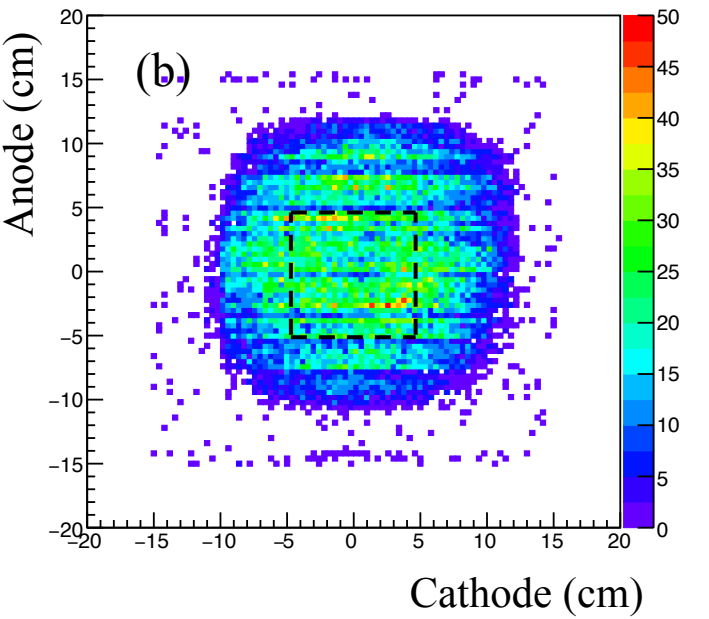
(b)
Anode (cm)
Cathode (cm)
20
15
10
5
0
−5
−10
−15
−20
50
45
40
35
30
25
20
15
10
5
0

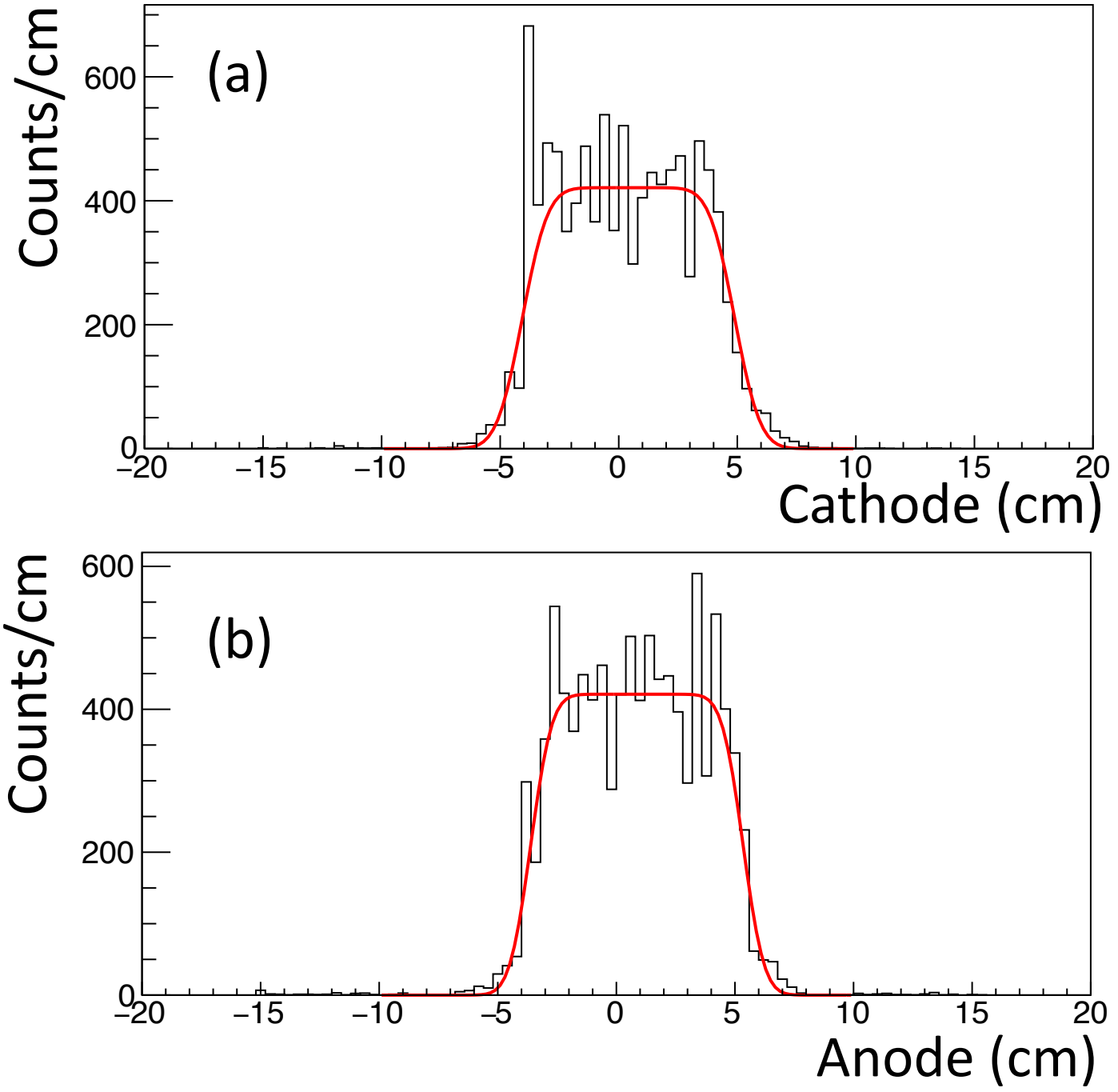
(a)
Counts/cm
600
400
200
0
−20
−15
−10
−5
0
5
10
15
20
Cathode (cm)
(b)
Counts/cm
600
400
200
0
−20
−15
−10
−5
0
5
10
15
20
Anode (cm)

Figure9

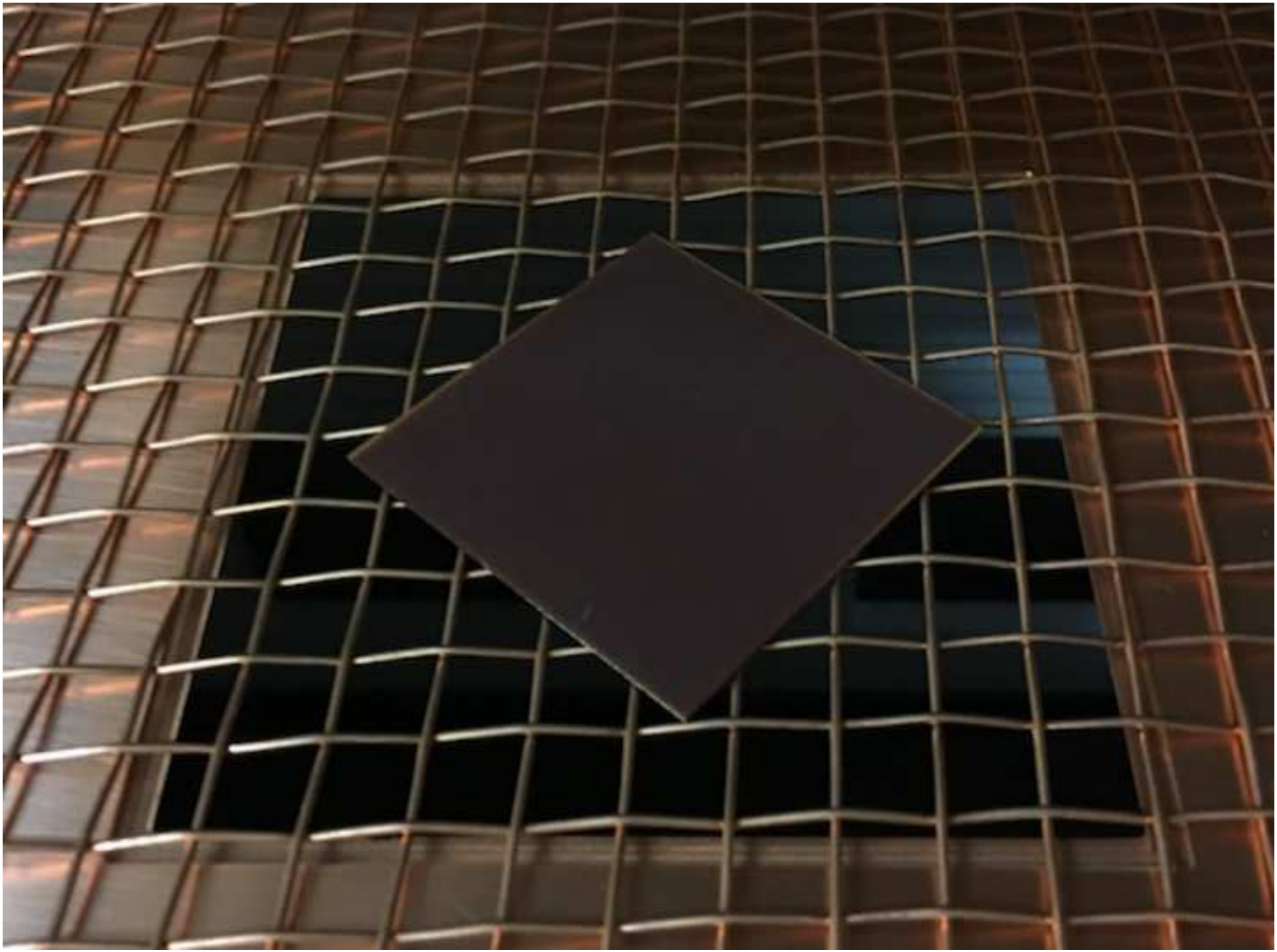

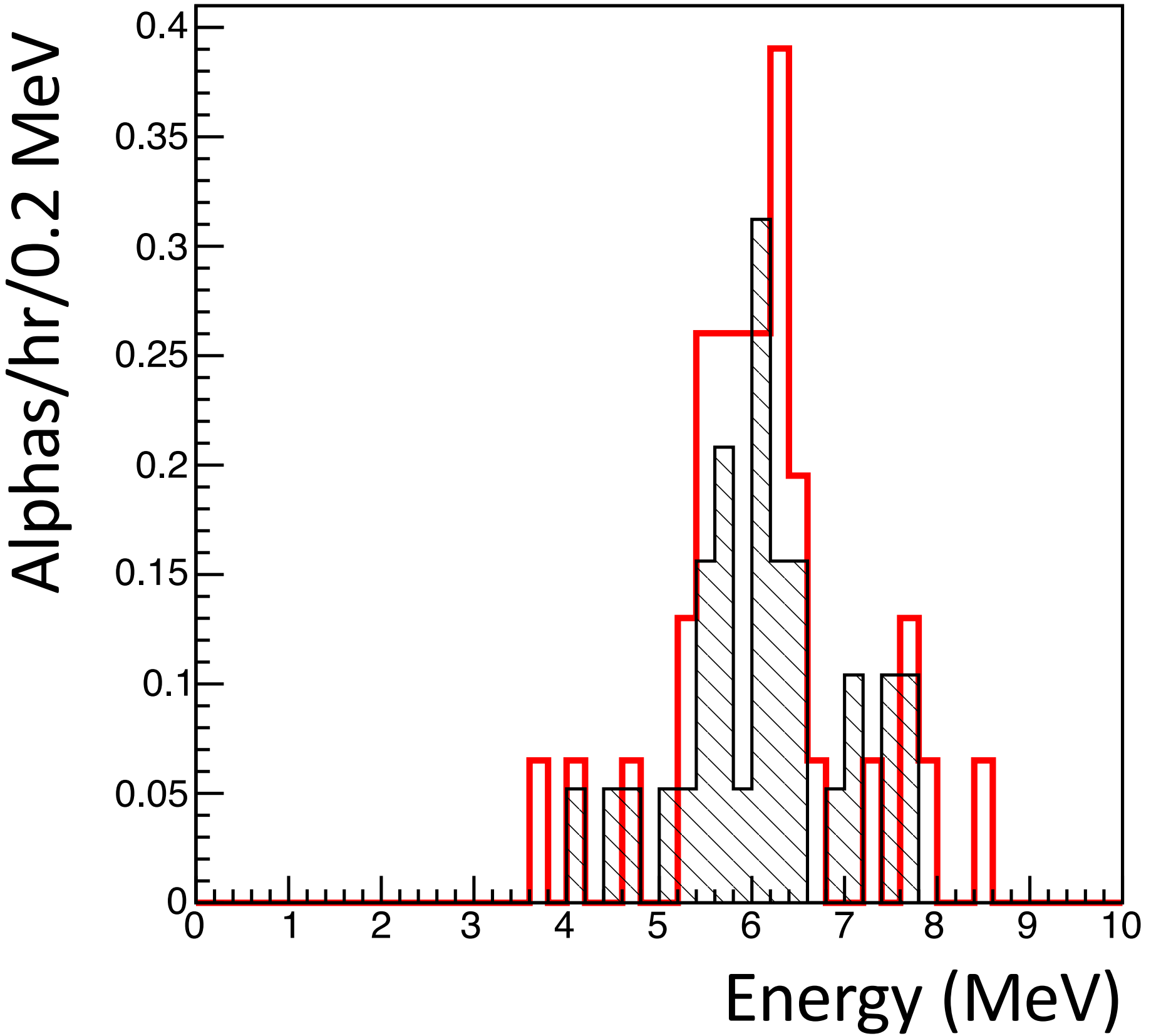
Alphas/hr/0.2 MeV
0.4
0.35
0.3
0.25
0.2
0.15
0.1
0.05
0
0
1
2
3
4
5
6
7
8
9
10
Energy (MeV)

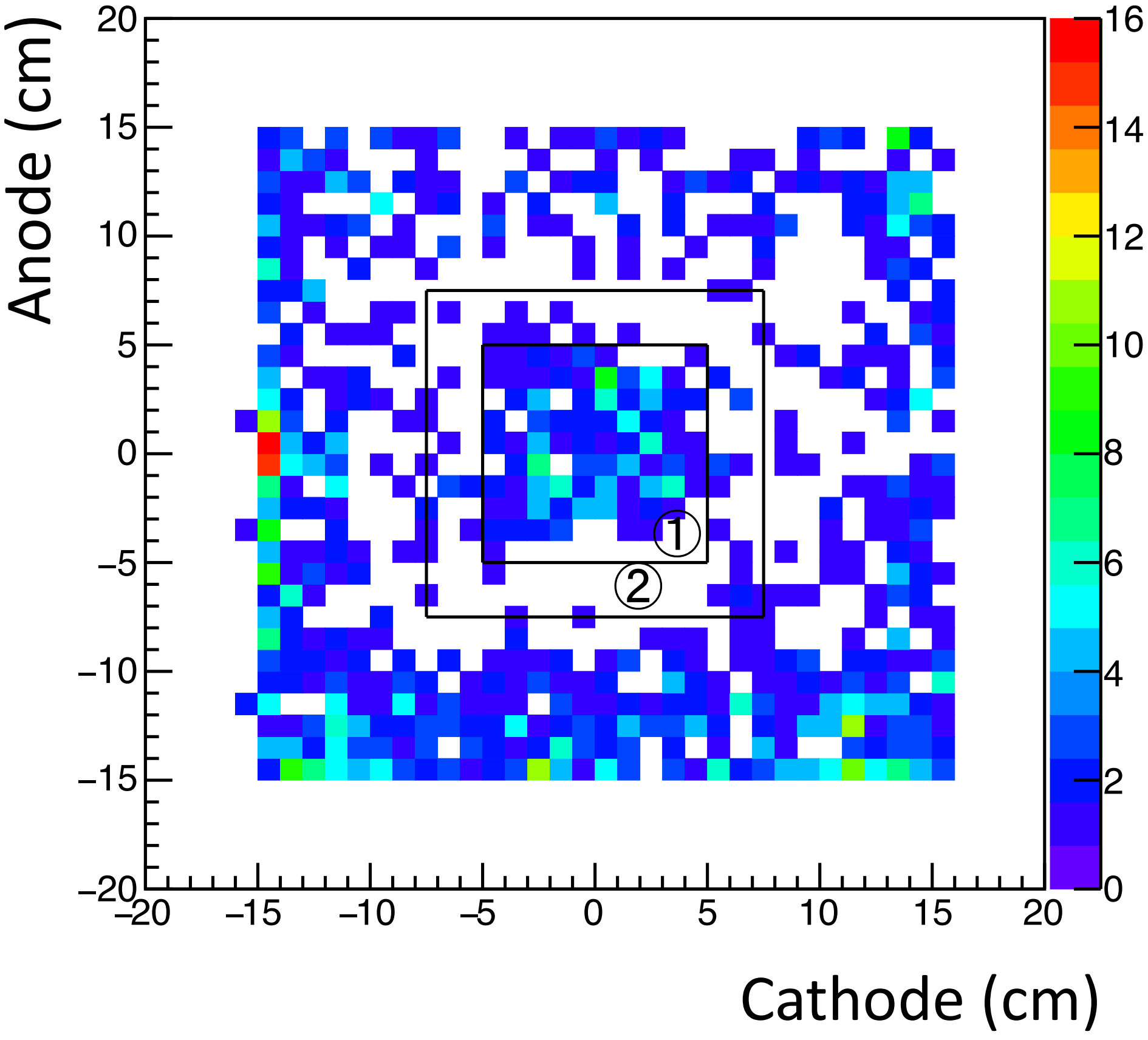
Anode (cm)
Cathode (cm)
20
15
10
5
0
−5
−10
−15
−20
−20
−15
−10
−5
0
5
10
15
20
16
14
12
10
8
6
4
2
0
1
2

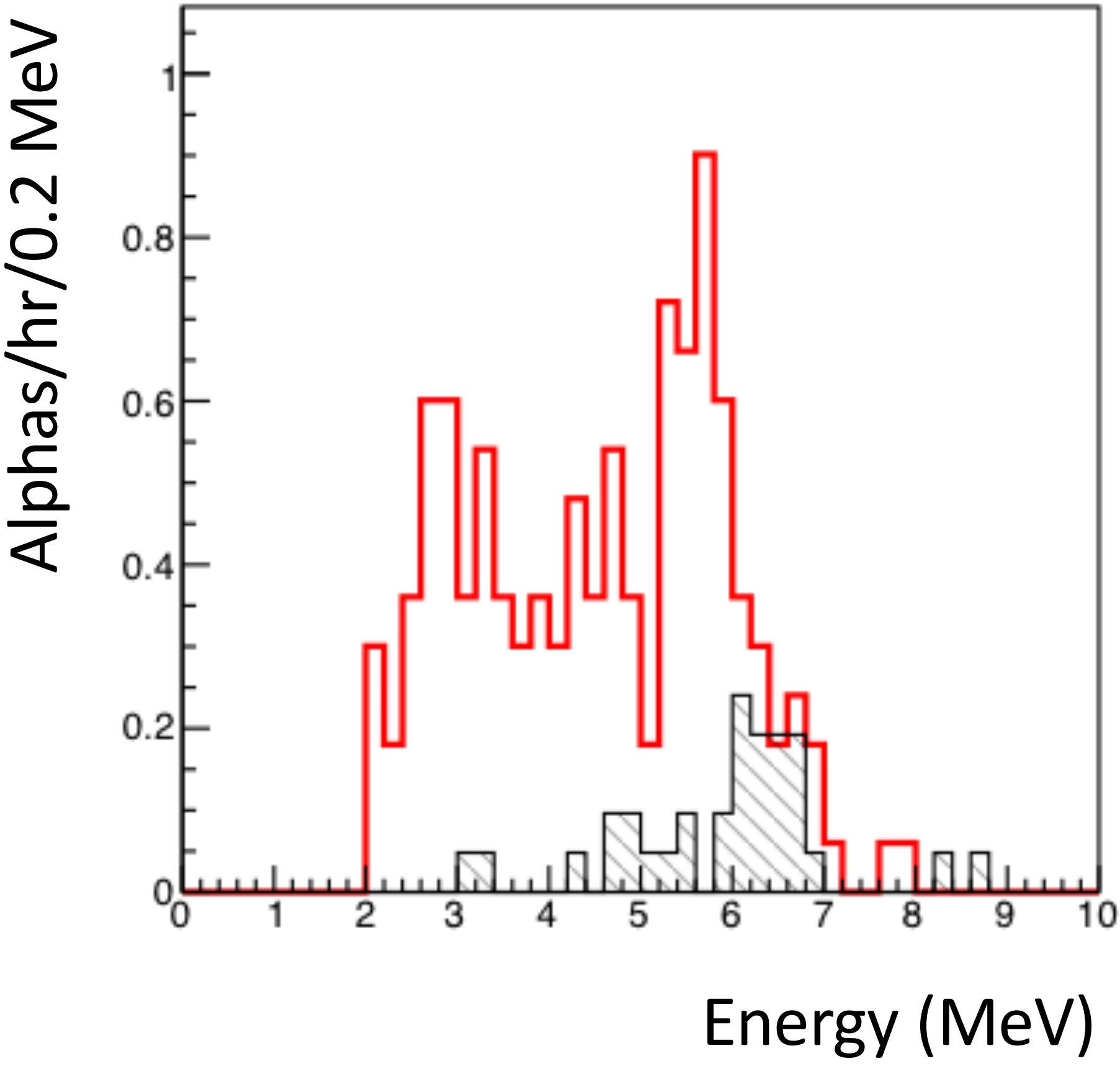
Alphas/hr/0.2 MeV
1
0.8
0.6
0.4
0.2
0
0
1
2
3
4
5
6
7
8
9
10
Energy (MeV)

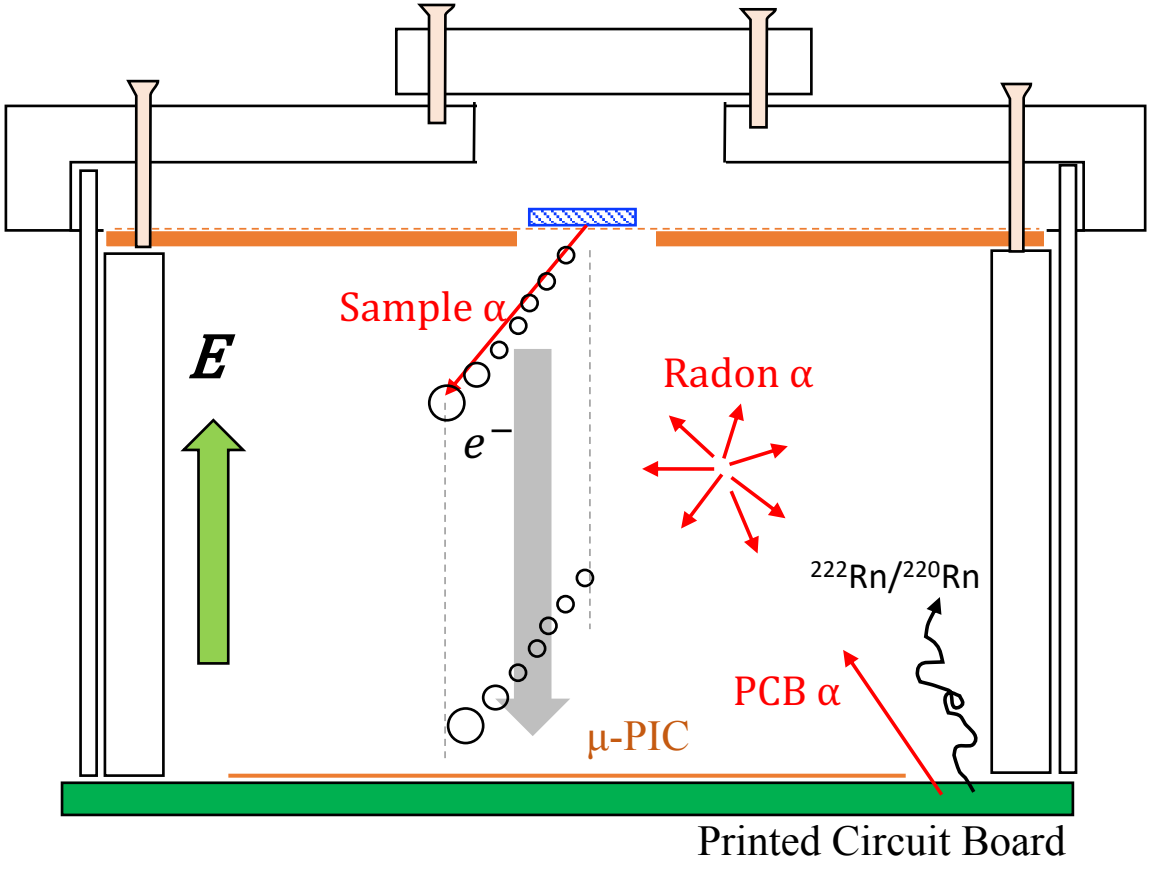
Sample α
E
Radon α
e⁻
222Rn/220Rn
PCB α
μ-PIC
Printed Circuit Board

	This work	HPGe detector
Sample volume (cm)	$(5 \times 5) \times 0.098$	$(5 \times 5) \times 2.47$
Sample weight (g)	6.8	169.5
Measureing time (hr)	75.85	308
Net α rate (α/cm^2/hr))	$(3.57^{+0.35}_{-0.33}) \times 10^{-1}$	—
^{232}Th impurities (ppm)	6.0 ± 1.4	5.84 ± 0.03
^{238}U impurities (ppm)	3.0 ± 0.7	2.31 ± 0.02

Table 1: Comparison of Screening result with this work and HPGe detector.

Dear Reviewer #1,
Thank you for your advices and suggestions. We attached files, corrected manuscript and difference. The corrected sentences have been indicated as a red with remove-line (old) and blue (new) one.

Abstract:
Line 2: detector material → detector materials
>> It was revised from "detector material" to "detector materials" in abstract, line 2.

Line 3: radioactive impurity → radioactive impurities
>> It was revised from "radioactive impurity" to "radioactive impurities" in abstract, line 3.

Line 3: isotopes in the → isotopes of the
>> It was revised from "in" to "of" in abstract, line 3.

Line 4: of surface radioactiviy: An alpha-particle → of surface and bulk radioactivity: Focused on the first one, an alpha-particle
>> It was added "and bulk" in abstract, line 4, and it was revised from "An alpha-particle" to "Focused on the first one, an alpha-particle" in abstract, line 4.

1. Introduction
Line 3: nonbarionic → non-barionic
>> It was revised from "nonbarionic" to "non-baryonic" in line 3.

Line 5-6: no direct detection of dark matter has yet been reported → any direct detection has yet been detected
>> It was revised to "any direct detection has yet been detected" in line 5.

Line 8-12: Although the DAMA group has observed the annual modulation with a significance of 9.3σ as the dark matter contribution [1], other groups such as XENON1T[2] and LUX [3] did not reproduced the signal. →Although the DAMA group has observed the annual modulation of dark matter particles in the galactic halo with a significance of 9.3σ [1], other groups such as XENON1T[2] and LUX [3] did not reported compatibles results.
>> The sentence was corrected from
"Although the DAMA group has observed the annual modulation with a significance of 9.3σ as the dark matter contribution [1], other groups such as XENON1T[2] and LUX [3] did not reproduced the signal."
to
"Although the DAMA group has observed the annual modulation of dark matter particles in the galactic halo with a significance of 9.3σ [1], other groups such as XENON1T[2] and LUX [3] did not report compatibles results." in line 8-12.

Line 18-19: (micro-TPC) and the main background is surface alpha particles → (micro-TPC), being the main background surface alpha particles
>> It was revised to "(micro-TPC), being the main background surface alpha particles" in line 18-19.

Line 20: material → materials
>> It was revised to "materials" in line 20.

Line 24: (it is its own → (i.e. it is its own
>> It was revised to "(i.e. it is its own antiparticle)" in line 24.

Line 25-26: and provides the absolute neutrino mass → REMOVE
>> It was removed.

Line 26-29: The GERDA ... yet to be observed → Experiments like GERDA [6] and KamLAND- Zen [7] have been able to set a lower limit on the half-life over 10^{25} yr at 90%CL by using 76 Ge and 136 Xe, respectively, but no positive signal of the 0νββ process has not be observed yet.
>> It was revised to "Experiments like GERDA [6] and KamLAND-Zen [7] have been able to set a lower limit on the half-life over 10^{25} yr and 10^{26} yr at 90%CL by using ^{76}Ge and ^{136}Xe, respectively, but no positive signal of the 0νββ process has not be observed yet" in line 25 -30.
The reference of KamLAND-Zen was changed to "A. Gando, et al., Phys. Rev. Lett. 117, 082503 (2016)" in line 500.

Line 32: precedes the measurement with at → set lower limits at
>> It was revised to "set lower limits at" in line 37.

Line 33 and 34: $T_{1/2} \rightarrow T_{1/2}(0\nu\beta\beta)$
>> It was revised to "$T_{1/2}(0\nu\beta\beta)$" in line 38 and 39.

Line 35-36: and a contamination of ^{208}Tl and ^{214} Bi in the detector dominates the background → for this experiment background is dominated by the ^{208}Tl and ^{214}Bi contamination present in the double beta emitter source foils
>> It was revised to "for this experiment background is dominated by the ^{208}Tl and ^{214}Bi contamination present in the double beta emitter source foils" in line 40-42.

Line 38: impurities with sensitivity → impurities in these foils with a sensitivity
>> It was revised to "impurities in these foils with a sensitivity" in line 44.

Line 46: material → materials
>> It was revised to “materials” in line 53.

Line 55-57: For example, the impurities might be contaminated to the electrodes in a pattern making process→ For example the impurities can be in a particular location due to the manufacturing process.
>> It was revised to “For example the impurities can be in a particular location due to the manufacturing process” in line 62-64.

Line 68-69: the study is concluded → main conclusions are presented
>> It was revised to “main conclusions are presented” in line 76.

2. Alpha-particle imaging detector based on gaseous micro-TPC
Line 77: μ -PIC, a gas circulation → μ -PIC as readout, a gas circulation
>> It was revised to “ μ -PIC as readout, a gas circulation “ in line 85.

Line 79: stainless-vessel → stainless-steel vessel
>> It was revised to “stainless-steel vessel” in line 87.

2.1 Setup and configuration
This section requires a complete revision including more details about some of the components and the associated discussion.
>> Thank you for your suggestions, and we answered your all questions in this subsection.
For example:
- Drift plane: What is the thickness?
The thickness is 1 mm. The drift plate has a size of (35 cm × 35 cm) × 0.1 cm, surface with electro-polished, and 9.5 cm × 9.5 cm hole. So that, the sentence was revised from “An oxygen-free copper plate with a surface polished to a roughness of 0.4 μm was used as the drift plate” to “An oxygen-free copper plate with a surface electro-polished to a roughness of 0.4 μm and with a size of (35 cm × 35 cm) × 0.1 cm was used as the drift plate” in line 94-97.
- Mesh: Thickness of the wires? Pitch (holes size)? Transparency? How could the transparency affects on the detection efficiency since it could stop alphas?
>> The mesh was made of 1mm-ϕ wire in 1cm pitch. Aperture ratio for alpha rays is calculated to 0.81. Since this ratio have already include to detection efficiency, the paper’s efficiency is not changed. In line 98-102, the sentence was revised from “A copper mesh was set on the drift plate to hold the sample at the window area, as shown in Fig. 3” to “A copper mesh made of 1-mm-ϕ wire in 1-cm pitch (aperture ratio of 0.81) was set on the drift plate to hold the sample at the window area, as shown in Fig. 3”.

- The pressure was set at 0.2 bar as a result of the optimization between the expected track length and the detector stability... → Any reference that supports this? If not more details are needed

>> Authentic CF_4 pressure is 0.1 bar [5] and 0.2 bar [12]. At 0.1 and 0.2 bar, 5-MeV alpha ray runs to ~16 cm and ~8cm in typical, respectively. The detector height is ok, but alpha ray goes out of μ-PIC area when alpha with length of 16 cm is emitted from edge of sample region (10 cm × 10 cm) in a case of 0.1 bar. We adopted pressure of 0.2 bar considering efficiency.

Figure 1 caption: Photographic of detector → Photography of the experimental setup

>> It was revised to "Photography of the experimental setup".

Figure 1 caption: A more detailed caption would be advisable.

>> We added

"The detector system is composed of a micro-TPC, a gas circulation system, and electronics. The stainless-steel vessel is uncovered so that the outer view of the TPC field cage can be viewed" in Fig. 1 caption.

Figure 2 caption: Indicate the field cage would be advisable.

>> Thank you for your advice. We added illustration of field cage copper wire in Teflon wall in Fig. 2, and you can see bottom figure. And the caption was revised to "Schematic cross section of detector setup. Sample window size is 9.5 cm × 9.5 cm. Electric field is formed by a drift plate biased at -2.5 kV and copper wires with 1 cm pitch connecting with chain registers".

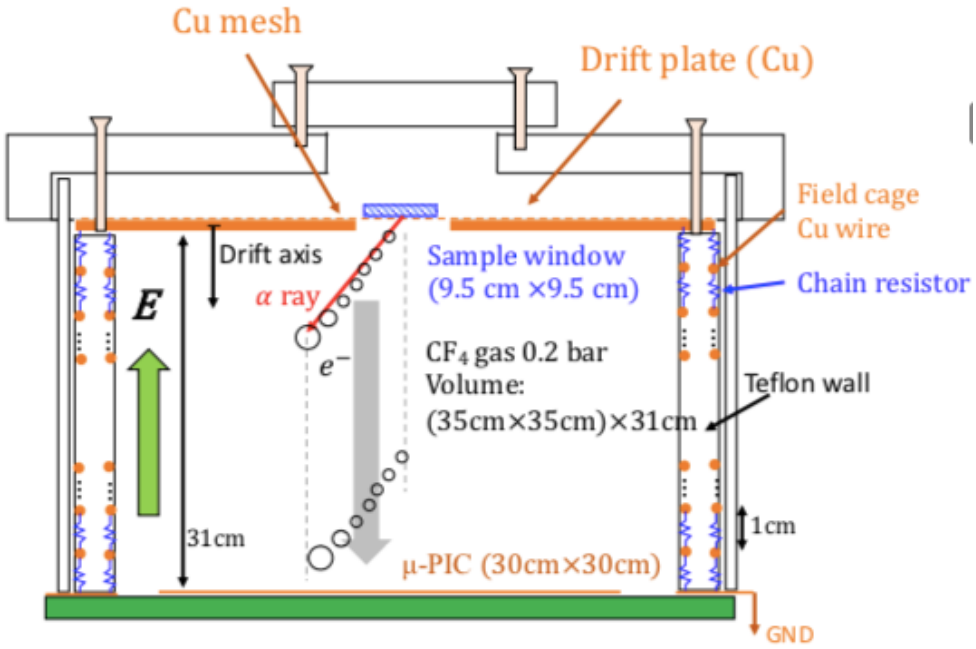

2.3 Gas circulation system

Line 122: protect a against → Not understandable: Rewrite

>> The paragraph of "A gas circulation system that uses activated charcoal pellets was developed for radon-background suppression and to protect a against gain deterioration due to the outgassing." was changed to "A gas circulation system that uses activated charcoal pellets (Molsievon, X2M4/6M811) was developed for following purposes: a suppression of radon background and a prevention of gain deterioration due to the outgassing" in line 134-138.

Line 124: circulate meter → Flow-meter

>> It was revised to "flow-meter" in line 139.

Line 126-129: The gas pressure was monitored to ensure the stable operation of the circulation system and as maintained within an increase of ~ 2% for several weeks. → The gas pressure was monitored to ensure the stable operation of the circulation system, operating within a variation of ~ 2% for several weeks.

>> Thank you for your suggestion. Another reviewer also suggestion it. The sentence was revised from

"The gas pressure was monitored to ensure the stable operation of the circulation system and as maintained within an increase of ~ 2% for several weeks"

to

"The gas pressure was monitored to ensure the stable operation of the circulation system, operating within ±2% for several weeks" in line 141-143.

Line 145-148: However, because the alpha particles were expected to be emitted from the sample, the drift-along coordinate of the emission point was assumed to be the position of the drift plate.

→ More discussion is advisable for this sentence. Why this assumption is true?

>> Thank you for your advice. The paragraph means to make event display because the detector aims to detect alpha rays emitted from sample. That assumption was used to reconstruct the alpha track, but this phrase "assumed" is inadequate in the sentence. So that, in line 155-162, the paragraph was revised from

"With this way of triggering … was assumed to be the position of the drift plate."

to

"The trigger is occurred when the electrons closest to the detection plane (indicated with the largest circle (e^-) in Fig.2) reach the μ-PIC. Since the main purpose of the detector is the alpha particle from the sample, the emission position of the alpha particle in the anode-cathode plane was determined at the position most distant from the μ-PIC in the track (the smallest circle in Fig. 2)".

Is there any reference talking about mean free path of alphas in gas?
>>The mean free path of 5 MeV alpha particle is ~8 cm and ~16 cm in 0.2 and 0.1 bar CF_4 gas, respectively. We added "The range of 5 MeV alpha particle is ~8 cm in 0.2 bar CF_4 gas, which would provide a reasonable detection efficiency considering the detector size." in line 113-116.

3. Performance check

3.2. Energy calibration

The whole point requires a major revision including Figure 4. Some questions to address: What is the used fit? Gaussian? Landau+Gaussian?
>>The Gaussian fitting around the peak is used. The red line as Gaussian fitting was added to Fig. 4. In the Fig.4 caption, we added "Red line is a fit result with a Gaussian."
How was the Energy scale in Figure 4 obtained? It has been included after calibration? It would be more representative to leave ADC counts. If the energy axis is left some discussion about quenching etc is required
>> It was obtained energy scale because the alpha-ray energy of source is known to 5.3 MeV. The calibration factor is 4.23 MeV/nC.
The sentences was revised from "alpha-particle source" to "alpha-particle source (5.3 MeV)" in line 176.
We revised the sentence from "The energy was calculated from the flash ADC waveform." to "The energy was converted from the charge integrated the voltage in time of flash ADC" in line 176-178.

The charge scale was added in Fig.4.

Since the charge peak was set to known energy of alpha-ray (5.3 MeV), the alpha-particle equivalent is used as energy unit "MeV" in this paper. We added "In this paper, the alpha-particle equivalent is used as the energy unit, MeV." in line 178-179.

Vertical axis of Figure 4 should be Counts / N MeV (or / N ADC units if the horizontal axis is changed)
>> We changed y-axis scale from "counts/bin" to "counts/MeV" in Fig. 4.

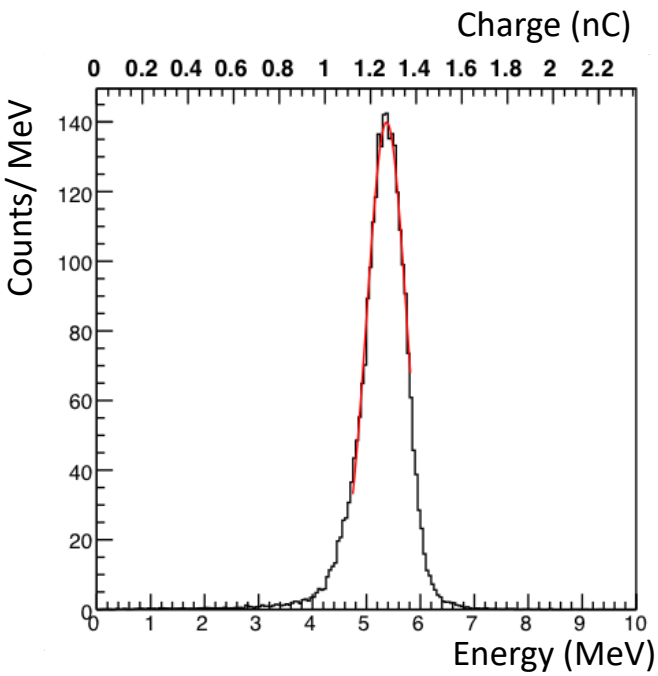

3.3. Event reconstruction

Line 176-177: The open circles are data → The open circles correspond to hits registered in data

>> It was revised to "The open circles correspond to hits registered in data" in line 193-194.

Line 194: is a number → is the number

>> It was revised to "is the number" in line 211.

Line 196-197: shift, and rotation and the angle→ shift, the rotation angle

>> It was revised to "shift, the rotation angle" in line 213-214.

Line 201: determining → determine

>> It was revised to "determine" in line 218.

Line 202: is a bit confusing to understand the direction $\theta = 90^{o}$, please clarify using $\theta = 90^{o}$ (i.e. parallel/perpendicular to the m-PIC plane)

>> the phrase of " $\theta = 90^{o}$" was revised to " $\theta = 90^{o}$ (i.e. parallel or perpendicular to the μ-PIC plane)" in line 219-220.

Line 203: sample → REMOVE

>> It was removed.

3.4. Track-sense determination

Line 208: as → a's check it and change it all along the text.

>> It was revised to " α 's" in line 226, 228, 230, 231, 234, 235, 260, 422, 429, 432, 434.

Line 213: are the μ-PIC and the directions are mostly → is the μ-PIC so the directions of a's coming from this component are mostly

>> It was revised to "is the μ-PIC so the directions of a's coming from this component are mostly upward-oriented" in 231.

Line 232: How t_p is determined? Are the registered pulses fitted? An explanation to this question is necessary

>> t_p is determined simply as a time when the voltage is the highest in region between t_0 and t_1 because of a rapid calculation. So that, we added sentence "t_p is a time when the voltage is the highest in region between t_0 and t_1." in line 253-255.

Line 240: F_{dwn} has two peaks → This is a strong statement looking at Figure 6. rewrite this sentence in a more conservative way.
>> The sentence was revised from "i.e., F_{dwn} has two peaks" to "i.e., F_{dwn} has two components of upward- and downward-oriented" in 261-262.

Line 245-248: The selection efficiency of $F_{dwn} > 0.5$ was estimated to be 0.964 ± 0.004 in the source-α spectrum while the radon background was reduced to half
→Why $F_{dwn} > 0.5$ has been chosen? Does it provides the best efficiency values? If this is the explanation an scanning of the Efficiency vs F_{dwn} should have been done, please add information about that.
>> You can see right figure which is a relation between the F_{dwn} threshold and efficiency. Left figure is a same of Fig. 6. The back and blue line are downward- and upward-oriented alpha ray's efficiency. The threshold was not optimized in best, but the reason why threshold of F_{dwn}=0.5 is set is to reject upward alpha (85%) and to select downward alpha (96%) efficiently.
The figure (b) was added in Fig. 6 and the caption of "(b) Efficiency of downward-(black solid) and upward-oriented (blue dashed) events as a function of F_{dwn} threshold." was added.
In the line 255-256, "Figure 6 shows typical F_{dwn} distribution" was changed to "Figure 6 (a) shows typical F_{dwn} distribution". And, "Figure 6 (b) shows the efficiency related on F_{dwn} threshold for downward-(black solid) and upward-oriented (blue dashed)" was added in the line 267-269.

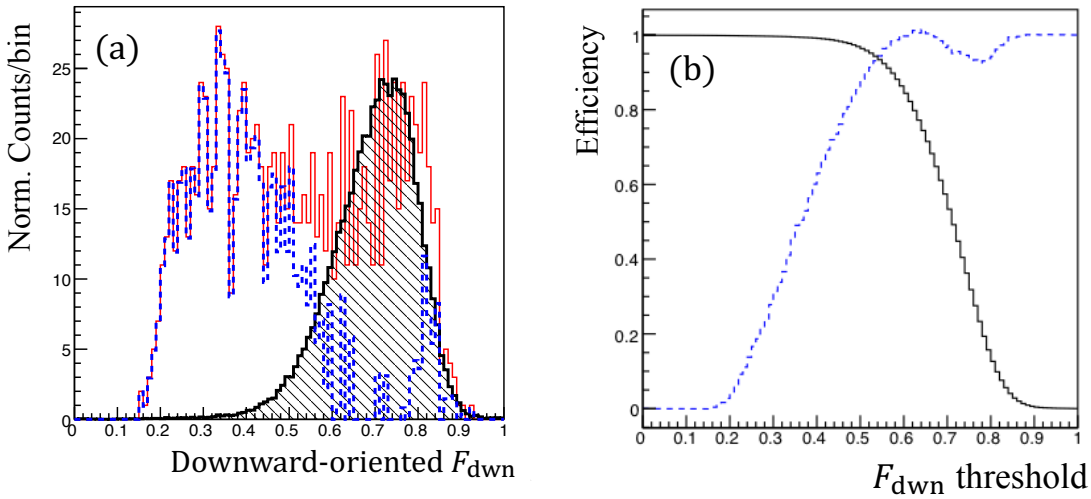

Lines 267-273: An additional figure illustrating the projections and the fits done to obtain the quoted resolution must be included.

>> The evidence to estimate position resolution shows in Fig. 8, which was added to the manuscript. You can see bottom plot. The histograms mean anode and cathode projections for alpha emit position. (a) and (b) represent cathode and anode, respectively. Since the Fig. 8 was added, a figure number of downstream was shifted to Fig. 8→9, Fig. 9→10, Fig. 10→11, Fig. 11→12, Fig. 12→13. Then, Fig. 11 and Fig. 12 were changed by your suggestion later.

Figure 8 caption is "Alpha-particle emission position projected to cathode (a) and anode (b). Red lines represent fitting with error functions."

In line 294-298, "as shown in Fig. 8. Figure 8 (a) and (b) represent the alpha-particle emission position projection to cathode and anode, respectively. The red lines are the fitting based on the error functions" was added.

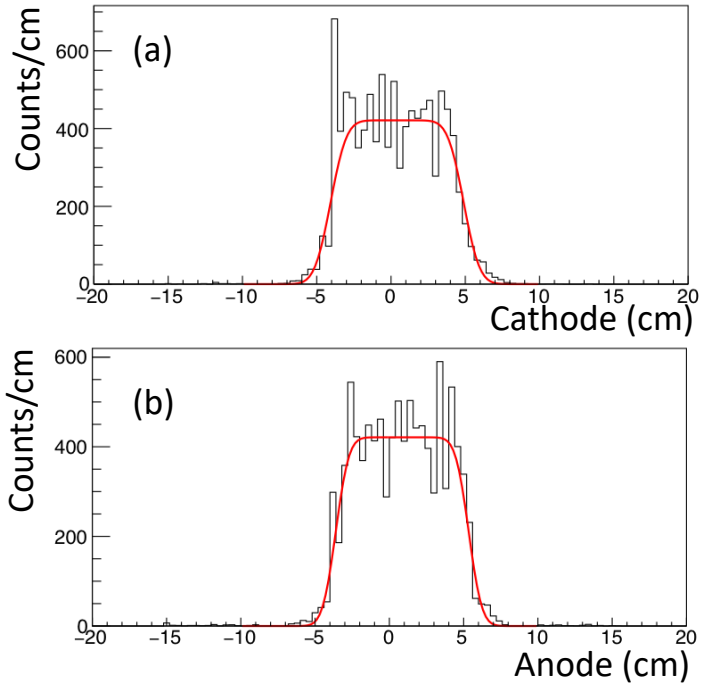

3.6 Efficiency of event selection → It is empty!!! please revise indexing

>> Sorry, it is our mistake. It was removed.

3.7 Detection and selection efficiency

Line 304: and thus the it was negligible → considering it negligible

>> It was revised to "considering it negligible" in 329.

Line 311: radioactivity and the statistic error is negligible → radioactivity, being the statistical error negligible

>> It was revised to "radioactivity, being the statistical error negligible" in line 335-336.

3.8.1 Setup

Line 317: The setup → A photograph of the sample position over the setup mesh
>> It was revised to "A photograph of the sample position over the setup mesh", in line 342-343.

Line 318: The live time → The measurement live time
>> It was revised to "The measurement live time", in line 344.

Line 342: is consistent → is compatible at less than 1 σ (Based on the numbers provided in lines 339 and 340 both values are compatible at 0.84 σ)
>> It was revised to "is compatible at less than 1 σ " in line 369.

Figure 9: If I understood correctly from the text, spectra correspond to upward-oriented alpha- particles. Please check
>> The caption in Fig. 9 (shifted to Fig. 10) was corrected from "Downward-oriented alpha-particle energy spectra…" to "Upward-oriented alpha-particle energy spectra …".

Line 377: How long were the measurements using HPGe detector? It MUST be indicated for further sensitivity discussion.
>> It is 308 hr measuring time. We added "with the measuring time of 308 hr" after "…using HPGe detector", in line 412.

Figure 10 and 11 should be changed in order
>> Thank you for your suggestion, and Fig. 10 (shifted to Fig. 11) and 11 (shifted to Fig. 12) were changed.

Figure 10: Why region 1 (sample) has the same orientation than region 2 (drift plate hole)? Looking the photography of Figure 8 sample is rotated with respect to whole. An explanation about this must be include in the text (section 3.8.3)
>> I am sorry to have confused you. The region ① indicates the sample window (9.5 cm × 9.5 cm hole). Although the sample set to turn 45 degree, it is no problem because the sample is completely within region ①. So, we revised the sentence from "The regions ① and ② are sample and background regions, respectively" to "The regions ① and ② are defined as sample and background regions, respectively. The sample region corresponds to the sample window" in line 389-392.

4. Discussion

Line 391: Add units to 3 x 10^{-3}
>> The unit "a/cm2/hr" was added in line 428.

Line 405: detection area → detection area, limited by the μ-PIC
>> It was revised to "detection area, limited by the μ-PIC" in line 443.

Line 434-435: with the one by another measurement → with the one obtained by a measurement done with a HPGe detector
>> It was revised to "with the one obtained by a measurement done with a HPGe detector" in line 477-479.

To have a more clear idea of the potential of this detector a more detailled discussion putting together the uncertainties of the measurement and the measurement times with the alpha detector and the HPGe detector must be included. Taking from the text results are:
Time μ-PIC: 75.85 hours
HPGe: ??
232Th m-PIC: 6.0 +/- 1.4 ppm
HPGe: 5.84 +/- 0.03 ppm 238U
μ-PIC: 3.0 +/- 0.7 ppm HPGe: 2.31 +/- 0.02 ppm
>> We added a table 1 summarized a result to measure the sample. Here, The detector aim to measure sample with α/h/cm2 than that with ppm.

	This work	HPGe detector
Sample volume (cm)	$(5 \times 5) \times 0.098$	$(5 \times 5) \times 2.47$
Sample weight (g)	6.8	169.5
Measureing time (hr)	75.85	308
Net α rate (α/cm^2/hr))	$(3.57^{+0.35}_{-0.33}) \times 10^{-1}$	—
^{232}Th impurities (ppm)	6.0 ± 1.4	5.84 ± 0.03
^{238}U impurities (ppm)	3.0 ± 0.7	2.31 ± 0.02

Table 1: Comparison of Screening result with this work and HPGe detector.

Dear Reviewer #2,

Thank you for your advices and suggestions. We attached files, corrected manuscript and difference. The corrected sentences have been indicated as a red with remove-line (old) and blue (new) one. I think your advices and suggestions make to be a good paper our manuscript.

Line 3, abstract, change to "impurities" since referring to multiple impurities
>> We changed “impurity” to “impurities” in line 3 in abstract.

Introduction, second paragraph, it seems there should be reference to more comprehensive studies of contamination in $0\nu\beta\beta$ experiments such as those in EXO-200 or Majorana Demonstrator assay papers.
>> “The $0\nu\beta\beta$ background has been well investigated as radioactive impurities such as ^{238}U and ^{232}Th decay-chain isotopes, ^{40}K, ^{60}Co, ^{137}Cs including in the detector material, which emit γ with around MeV [EXO, MAJO]” was added in line 32-37, where these references represent follows:
[EXO] D. S. Leonard, et al., Nucl. Instr. Meth. A 871 (2017) 169.
[MAJO] N. Abgrall, et al., Nucl. Instr. Meth. A 828 (2016) 22.

Line 12, change to "reproduce"
>> Thank you for your advice. The sentence was revised significantly according to another reviewer’s suggestion from
“Although the DAMA group has observed the annual modulation with a significance of 9.3σ as the dark matter contribution [1], other groups such as XENON1T[2] and LUX [3] did not reproduced the signal.”
to
“Although the DAMA group has observed the annual modulation of dark matter particles in the galactic halo with a significance of 9.3σ [1], other groups such as XENON1T[2] and LUX [3] did not report compatibles results” in line 8-12.

Line 54, change "has not an" to "does not have a"
>> It was revised to "does not have a" in line 61-62.

Line 56, perhaps change "might be contaminated to" to "may be associated with"
>> Thank you for your suggestion. The sentence was revised according to another reviewer’s suggestion from
”For example, the impurities might be contaminated to the electrodes in a pattern making process”
to
”For example the impurities can be in a particular location due to the manufacturing process” in line 62-64.

Line 79, change to stainless-steel vessel
>> It was revised to “stainless-steel vessel” in line 87.

Line 83, shouldn't these units be cm?
Line 89, shouldn't these units be cm?
Line 151, shouldn't these units be cm?
Line 314, shouldn't these units be cm?
>> Thank you for your advice. These units were revised as follows:
“(35 × 35) × 31 cm^3“ to “(35 cm × 35 cm) × 31 cm”, in line 91.
“(35 × 35) × 0.1 cm^3“ to “(35 cm × 35 cm) × 0.1 cm”, in line 96.
“(9.5 × 9.5) cm^2“ to “9.5 cm× 9.5 cm”, in line 98, in Fig. 3 caption .
“10 × 10 cm^2” to “10 cm× 10 cm”, in line 199.
“5 × 5 cm^2” to “5 cm× 5 cm”, in line 387, Fig.9 caption.

Line 85, add the
>> It was revised to “at the Kamioka facility in the Institute for Cosmic Ray Research, Japan“ in line 92-94.

Line 86, how polished?
>> It is electro-polish, and the sentence was revised from “polished” to “electro-polished” in line 95.

Line 94, what is the source and purity of the CH4 gas?
>> The C4 gas is 5N grade, it means a purity of 99.999% or more. The sentence “(5N grade: a purity of 99.999% or more)” was added in line 104-105.

Line 96, perhaps sate the source of the copper since you mention later it contains U and Th.
>> The μ-PIC read line is made by plating copper. We measure the plating copper using HPGe detector, and it was found ^{238}U and ^{232}Th impurities are less than 0.13 and 0.06 ppm, respectively. So that, main source of alpha ray emitted from μ-PIC is understood as polyimide with glass fibers.

Line 101, change from "was" to "were"
>> It was revised to “were“ in line 112.

Line 122, remove "a"

>>Another reviewer suggests to rewrite the paragraph. The paragraph of “A gas circulation system that uses activated charcoal pellets was developed for radon-background suppression and to protect a against gain deterioration due to the outgassing.” was changed to “A gas circulation system that uses activated charcoal pellets (X2M4/6M811) was developed for following purposes: a suppression of radon background and a prevention of gain deterioration due to the outgassing” in line 134-138.

Line 128-129, perhaps simply state the desired pressure ± %

>> Thank you for your suggestion. Another reviewer also suggestion it. The sentence was revised from

“The gas pressure was monitored to ensure the stable operation of the circulation system and as maintained within an increase of ~ 2% for several weeks”

to

“The gas pressure was monitored to ensure the stable operation of the circulation system, operating within ±2% for several weeks” in line 141-143.

Lines 141-148, awkward wording, consider revising

>> Thank you for your advice. The paragraph means to make event display because the detector aims to detect alpha rays emitted from sample. That assumption was used to reconstruct the alpha track, but this phrase “assumed” is inadequate in the sentence. So that, the paragraph was revised from

“With this way of triggering … was assumed to be the position of the drift plate.”

to

“The trigger is occurred when the electrons closest to the detection plane (indicated with the largest circle (e^-) in Fig.2) reach the μ-PIC. Since the main purpose of the detector is the alpha particle from the sample, the emission position of the alpha particle in the anode-cathode plane was determined at the position most distant from the μ-PIC in the track (the smallest circle in Fig. 2)” in line 155-162.

Line 226, change "tack" to "track"

>> It was revised in 245.

Paragraph beginning at line 298 is awkward, please revise

>> We revised the sentence from

“For criterion C3, as shown in Fig. 7 (a), to reject the remained the radon and detector-αs, the selection region for alpha-particle emission point was set between -8.0 cm and 8.0 cm in both the anode and cathode coordinate.”

to

“For criterion C3, source-α was selected within a region ±8 cm in both the anode and cathode, as shown in Fig. 7 (a)” in the line 325-327.

Line 306, calculated to a detection efficiency of…

>> Thank you for your advice, and it was revised from

"The selection efficiency for C1, C2, and C3 containing the detection efficiency was $(2.17 \pm 0.29) \times 10^{-1}$ counts/a …"

to

"The selection efficiency for C1, C2, and C3 containing the detection efficiency was calculated to be $(2.17 \pm 0.29) \times 10^{-1}$ counts/a … " in line 330-332.

Line 310, uncertainty

>> It was revised in line 335.

Line 311, statistical

>> It was revised. Another reviewer also pointed it, and the sentence was revised from

"… the source radioactivity and the statistic error is negligible."

to

"… the source radioactivity, being the statistical error negligible" in line 335-336.

Line 323, in the region

>> it was revised "on the region" to "in the region" in line 349.

Line 326-330, this is confusing. It appears the background from one region was used to normalize the other region, and that result was checked by comparison of the two regions. This is a circular argument.

>> Thank you for your advice. We found the sentence "The net α rate from the sample was thus evaluated by subtracting the background rate from the rate of the sample region" repeated a previous sentence "The α rate of the sample was estimated by subtracting the background rate". We remove that sentence.

Then, at the sentence "It was necessary to confirm that the background rates in both regions were consistent with each other" was revised to "Typically, the upward and downward radon-α rates are same. The sample-α has mainly downward-oriented. Thus, the background rate in the sample region could be estimated by the upward rate in the sample region and independently cross-checked by the upward rate in the outer region" in line 352-357.

Line 372, the statement "Assuming the alpha spectrum is constituted only from 232Th or 238U, the impurity is estimated to be 6.0 ± 1.4 or 3.0 ± 0.7 ppm, respectively" comes out of nowhere with no explanation or how it was calculated. This needs elaboration.
>> Using Monte Carlo simulation, it was assumed isotope of U or Th include in sample uniformity. Then, the alpha rays emitted from U and Th decay-chain isotopes are simulated, and a prediction number of alpha rays related on the impurities quantities (ppm) is computed as a spectrum. The observed data is fitted by the spectrum as shown in bottom plot, where a free parameter is the normalization factor of spectrum. The error is determined to 68%CL in sigma. So, we revised the sentence from "Assuming the alpha spectrum is constituted only from ^{232}Th or ^{238}U, the impurity is estimated to be 6.0 ± 1.4 or 3.0 ± 0.7 ppm, respectively" to "Here, the impurity of ^{232}Th and ^{238}U is estimated by comparing with a prediction of α rate spectrum in the simulation, where it mentions that the isotope in the material is assumed as only ^{238}U or ^{232}Th because of the continuous α rate spectrum. In the fit region between 2 and 10 MeV, the impurity of ^{232}Th or ^{238}U is estimated to be 6.0 ± 1.4 or 3.0 ± 0.7 ppm, respectively." in line 402-409.

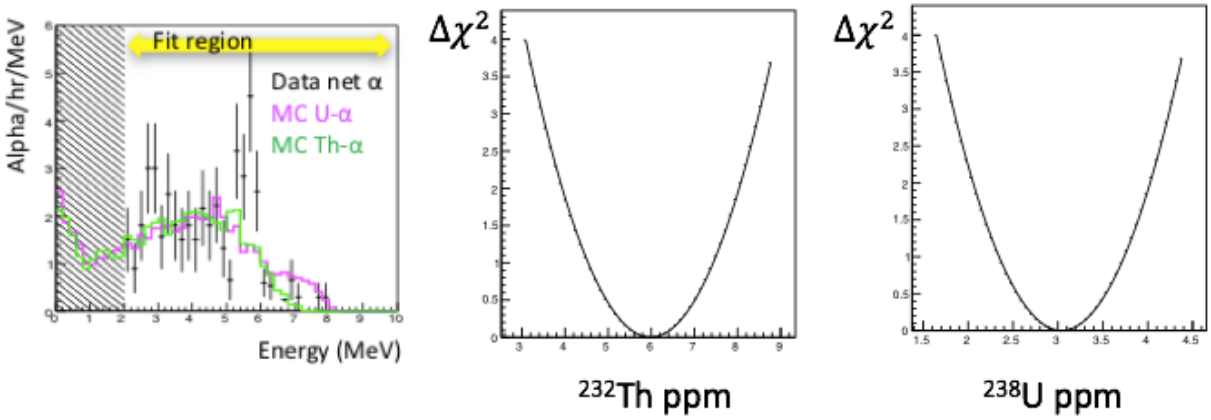

Line 391, units needed
>> It was revised from "σ ~3×10^-3" to "σ ~3×10^-3 a/cm^2/hr" in line 428.

Line 393, sample alphas?
>> Thank you for your advice. The phrase was revised from "radon-αs" to "sample-α's" in 429.

Line 394-398, the comparison of error rates and the impact to the sensitivity needs clarification here.
>> The paragraph was revised to "When the α rate (~1x10^{-3}a/cm^2/hr) as the same of the radon-α's (~1x10^{-3}a/cm^2/hr) was observed, the sum of squares of these σ's for the sample and radon-α's would be expected to be a few 10^{-3} α/cm^2/hr as the measurement limit by subtraction with these α rates" in line 430-436.

Line 414-415, this varies with radioisotope so such a statement needs to be more specific.
>> You are right. The estimate of ppb level was calculated by simulation of ^{238}U or ^{323}Th in 1mm-thick copper plate. The sentence “Here, this level was estimated as an assumption of ^{238}U or ^{232}Th in 1-mm-thick copper plate” were added in line 454-456.

Line 417, specify the cooling is for radon suppression and be specific regarding "material with less impurities".
>> We revised the sentence from “We can potentially improve the background rate by using the cooled charcoal and using a material with less impurities” to “We can potentially improve the background rate by using the cooled charcoal to suppress radon gas and using a material with less impurities such as polytetrafluoroethylene, polyimide, and polyetheretherketone without glass fibers” in line 456-461.

Line 422, sentence should read "With these improvements, the detector would achieve the performance goal".
>> Thank you for your advice, and it was revised from
“With these improvements, the detector would achieved the performance goal”
to
“With these improvements, the detector would achieve the performance goal” in 465-466.

A difference with revised one

Development of an alpha-particle imaging detector based on a low radioactive micro-time-projection chamber

H. Ito[a*], T. Hashimoto[a], K. Miuchi[a], K. Kobayashi[b,c],Y. Takeuchi[a,c], K. D. Nakamura[a],T. Ikeda[a], and H. Ishiura[a]

[a] *Kobe University, Kobe, Hyogo 657-8501, Japan.*

[b] *Institute for Cosmic Ray Research (ICRR), the University of Tokyo, Kashiwa, Chiba 277-8582 Japan.*

[c] *Kavli Institute for the Physics and Mathematics of the Universe (WPI), The University of Tokyo Institutes for Advanced Study, University of Tokyo, Kashiwa, Chiba 277-8583, Japan.*

Abstract

An important issue for rare-event-search experiments, such as the search for dark matter or neutrinoless double beta decay, is to reduce radioactivity of the ~~detector material~~detector materials and the experimental environment. The selection of materials with low ~~radioactive impurity~~radioactive impurities, such as isotopes ~~in~~of the uranium and thorium chains, requires a precise measurement of surface and bulk radioactivity. Focused on the first one, an~~An~~ alpha-particle detector has been developed based on a gaseous micro-time-projection chamber. A low-α μ-PIC with reduced alpha-emission background was installed in the detector. The detector offers the advantage of position sensitivity, which allows the alpha-particle contamination of the sample to be imaged and the background to be measured at the same time. The detector performance was measured by using an alpha-particle source. The measurement with a sample was also demonstrated and the sensitivity is discussed.

Keywords: Alpha-particle detector, Position sensitivity, Time projection chamber, μ-PIC, Low background

1. Introduction

Approximately 27% of the universe is dominated by ~~nonbarionic~~non-baryonic matter, called dark matter. Although many experimental groups have been searching for dark matter, ~~no direct detection of dark matter has yet been reported~~any direct detection has yet been detected. Typical experiments that search for dark matter are performed by using massive, low-background detectors. ~~Although the DAMA group has observed the annual modulation with a significance of 9.3σ as the dark matter contribution [1], other groups such as XENON1T [2] and LUX [3] did not reproduced the signal~~ Although the DAMA group has observed the annual modulation of dark matter particles in the galactic halo with a significance of 9.3σ [1], other groups such as XENON1T [2] and LUX [3] did not report compatibles results. Meanwhile, a direction-sensitive method has been focused because of an expected clear anisotropic signal due to the motion of the solar system in the galaxy [4]. The NEWAGE group precedes a three-dimensionally sensitive dark matter search with a micro-time-projection chamber ~~(micro-TPC) and the main background is surface alpha particles~~(micro-TPC), being the main background surface alpha particles from ^{238}U and ^{232}Th in the detector ~~material~~materials or in the μ-PIC [5].

Neutrinoless double beta ($0\nu\beta\beta$) decay is a lepton-number-violating process, which suggests the neutrino as a Majorana particle (i.e. it is its own antiparticle) ~~and provides the absolute neutrino mass. The GERDA [6] and KamLAND-Zen [7] groups recorded a lower-limit half-life over 10^{25} yr at 90%CL by using ^{76}Ge and ^{136}Xe, respectively,~~

*Corresponding author. E-mail address: ito.hiroshi@crystal.kobe-u.ac.jp (H. Ito).

~~and the $0\nu\beta\beta$ decay has yet to be observed~~ Experiments like GERDA [6] and KamLAND-Zen [7] have been able to set a lower limit on the half-life over 10^{25} yr and 10^{26} yr at 90%CL by using ^{76}Ge and ^{136}Xe, respectively, but no positive signal of the $0\nu\beta\beta$ process has not be observed yet. Conversely, a tracking system for two electrons provides strong evidence of the $0\nu\beta\beta$ decay process. The $0\nu\beta\beta$ background has been well investigated as radioactive impurities such as ^{238}U and ^{232}Th decay-chain isotopes, ^{40}K, ^{60}Co, ^{137}Cs including in the detector material, which emit γ with around MeV [8, 9]. The NEMO3 group ~~precedes the measurement with at~~set lower limits at $T_{1/2}(0\nu\beta\beta) > 2.5 \times 10^{23}$ yr (90%CL) for ^{82}Se [10], and $T_{1/2}(0\nu\beta\beta) > (1.1 - 3.2) \times 10^{21}$ yr (90%CL) for ^{150}Nd [11] ~~and a contamination of ^{208}Tl and ^{214}Bi in the detector dominates the background~~ for this experiment background is dominated by the ^{208}Tl and ^{214}Bi contamination present in the double beta emitter source foils. The SuperNEMO group has developed the BiPo-3 detector to measure the radioactive ~~impurities with sensitivity~~ impurities in these foils with a sensitivity less than 2 μBq/kg (90%CL) for ^{208}Tl and 140 μBq/kg (90%CL) for ^{214}Bi [12]. Therefore, the background of $0\nu\beta\beta$ decay is not only a contamination by the end point of continuous energy in an ordinary $2\nu\beta\beta$ decay process, but also the radiative impurities such as ^{238}U and ^{232}Th in the detector.

To estimate the radioactive impurities in the detector ~~material~~materials, the XMASS group measured ^{210}Pb and ^{210}Po in the bulk of copper by using a commercial alpha-particle detector (Ultra-Lo 1800, XIA) [13]. The alpha detector has a good energy resolution (as explained in Sec. 3.2) and a mechanism to reduce the background by waveform analysis, and thus a sensitivity is $\sim 10^{-4}$ α/cm^2/hr. However, it has no position sensitivity. A sample such as a micro pattern gas detector board ~~has not an~~does not have a uniform radioactive contamination. ~~For example, the impurities might be contaminated to the electrodes in a pattern making process~~ For example the impurities can be in a particular location due to the manufacturing process. Therefore, a position-sensitive alpha detector is required to select materials for the rare-event-search experiments

This paper is organized as follows. The details of the alpha-particle detector, setup, low-α micro pixel chamber (μ-PIC), gas circulation system, electronics, and trigger data acquisition system are described in Sec. 2. The performance check that uses the alpha-particle source, a sample test, and background estimation are described in Sec. 3. The remaining background of the detector and future prospects are discussed in Sec. 4. Finally, ~~the study is concluded~~ main conclusions are presented in Sec. 5.

2. Alpha-particle imaging detector based on gaseous micro-TPC

A new alpha-particle detector was developed based on a gaseous micro-TPC upgraded from the NEWAGE-0.3a detector [14] which was used to search for dark matter from September, 2008 to January, 2013. The detector consisted of the micro-TPC using a low-α μ-PIC as readout, a gas circulation system, and electronics, as shown in Fig.1. The TPC was enclosed in a ~~stainless-vessel~~stainless-steel vessel for the gas seal during the measurement.

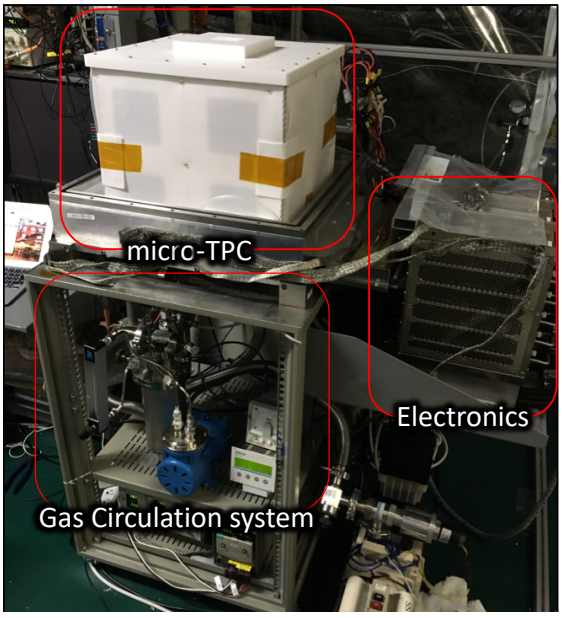

Fig. 1: ~~Photographic of detector~~ Photography of the experimental setup. The detector system is composed of a micro-TPC, a gas circulation system, and electronics. The stainless-steel vessel is uncovered so that the outer view of the TPC field cage can be viewed.

2.1. Setup and configuration

Figure 2 shows a schematic view of the detector, where the gas volume is ~~$(35 \times 35) \times 31$ cm^3.~~ (35 cm $\times$ 35 cm) $\times$ 31 cm.

The detector was placed underground at the Kamioka facility in the Institute for Cosmic Ray Research, Japan. An oxygen-free copper plate with a surface ~~polished~~ electro-polished to a roughness of 0.4 μm and with a size of (35 cm × 35 cm) × 0.1 cm was used as the drift plate. The drift plate had an opening with a size of ~~(9.5 × 9.5 cm^2)~~ 9.5 cm × 9.5 cm as a sample window. A copper mesh made of 1-mm-ϕ wire in 1-cm pitch (aperture ratio of 0.81) was set on the drift plate to hold the sample at the window area, as shown in Fig. 3. The electrons ionized by the alpha particles drift toward the μ-PIC with a vertical upward-pointing electric field E. CF_4 gas (5N grade: a purity of 99.999% or more), which was also used in the NEWAGE-0.3a, was used as the chamber gas because of the low diffusion properties. The pressure was set at 0.2 bar as a result of the optimization between the expected track length and the detector stability. The track length was expected to be longer, which improved the tracking performance when the gas pressures ~~was~~were low, while the discharge rate of the μ-PIC increased. The range of 5 MeV alpha particle is ~8 cm in 0.2 bar CF_4 gas, which would provide a reasonable detection efficiency considering the detector size. The electric field in the drift volume, $E = 0.4$ kV/cm/bar, was formed by supplying a negative voltage of 2.5 kV and placing field-shaping patterns with chain resistors every centimeter [15]. The drift velocity was 7.4 ± 0.1 cm/μs. The μ-PIC anode was connected to +550 V. The typical gas gain of μ-PIC was 10^3 at ~ 500 V.

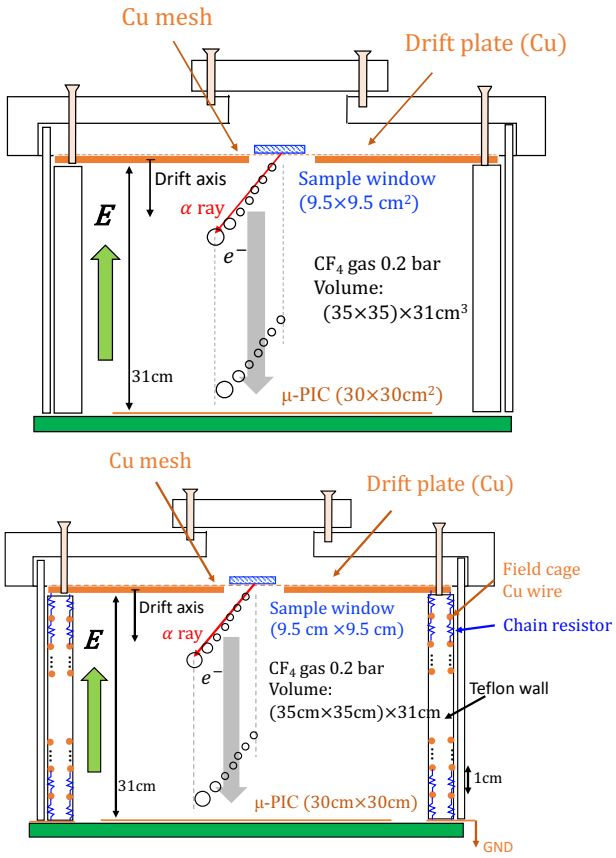

Fig. 2: (top figure is old. bottom one is revised.) Schematic cross section of detector setup. Sample window size is 9.5 cm × 9.5 cm. Electric field is formed by a drift plate biased at -2.5 kV and copper wires with 1 cm pitch connecting with chain registers.

2.2. Low-α μ-PIC

The background study for the direction-sensitive dark matter search suggests that μ-PIC has radioactive impurities of ^{238}U and ^{232}Th which emit alpha particles [5]. A survey with a HPGe detector revealed that μ-PIC's glass cloth was the main background source, and so the impurities were removed [16]. Details of the device with the new material, a low-α μ-PIC, will be described in Ref [17].

2.3. Gas circulation system

~~A gas circulation system that uses activated charcoal pellets was developed for radon-background suppression and to protect a against gain deterioration due to the outgassing.~~ A gas circulation system that uses activated charcoal pellets (Molsievon, X2M4/6M811) was developed for following purposes: a suppression of radon background and a prevention of gain deterioration due to the outgassing. A pump (EMP, MX-808ST-S) and a needle-type ~~circulate meter~~ flow-meter (KOFLOC, PK-1250) were used to flow the gas at a rate of ~ 500 cm^3/min. ~~The gas pressure was monitored to ensure the stable operation of the circulation system and as maintained within an increase of ~ 2% for several weeks~~ The gas pressure was monitored to ensure the stable operation of the circulation system, operating within ±2% for several weeks.

2.4. Electronics and trigger data acquisition system

The electronics for the μ-PIC readout consisted of amplifier-shaper discriminators [18] for 768 anode and 768 cathode signals and a position-encoding module [19] to reconstruct the hit pattern. A data acquisition system consisted of a memory board

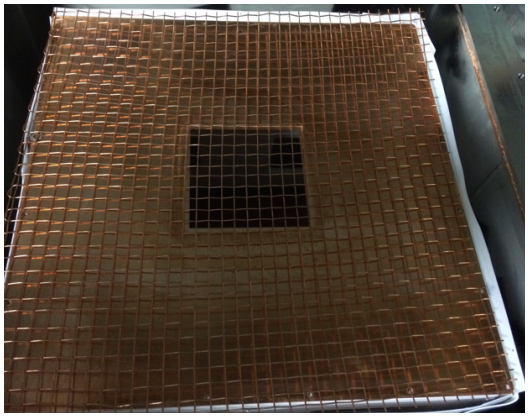

Fig. 3: Drift plate with a sample window (hole size is ~~9.5 × 9.5 cm²~~ 9.5 cm × 9.5 cm) and copper support mesh.

to record tracks and a flash analog-to-digital converter (ADC) for the energy measurement. The flash ADC with 100 MHz sampling recorded the sum signal of the cathode strips with a full time range of 12 μs. The anode sum signal issued the trigger. ~~With this way of triggering, in contrast to the trigger by signal (for example, primary scintillation) in the TPC before the drift, the absolute position along the drift direction cannot be measured. However, because the alpha particles were expected to be emitted from the sample, the drift-along coordinate of the emission point was assumed to be the position of the drift plate.~~ The trigger is occurred when the electrons closest to the detection plane (indicated with the largest circle (e^-) in Fig. 2) reach the μ-PIC. Since the main purpose of the detector is the alpha particle from the sample, the emission position of the alpha particle in the anode-cathode plane was determined at the position most distant from the μ-PIC in the track (the smallest circle in Fig. 2).

3. Performance check

3.1. Alpha-particle source

A ~~10 × 10 cm²~~ 10 cm × 10 cm copper plate with ^{210}Pb accumulated on the surface was used as an alpha-particle source for the energy calibration and energy-resolution measurement [13]. The source emits alpha particles with an energy of 5.3 MeV as a decay of ^{210}Po. The alpha-particle emission rate (hereinafter called the α rate) of the source plate was calibrated to be 1.49 ± 0.01 α s^{-1} for 4.8–5.8 MeV by using the Ultra-Lo 1800 [13].

3.2. Energy calibration

An energy calibration was conducted with the alpha-particle source (5.3 MeV). ~~The energy was calculated from the flash ADC waveform.~~ The energy was converted from the charge integrated the voltage in time of flash ADC. In this paper, the alpha-particle equivalent is used as the energy unit, MeV. Figure 4 shows a typical energy spectrum of the alpha-particle source. The energy resolution was estimated to be 6.7% (1σ) for 5.3 MeV, which is worse than the Ultra-Lo 1800 resolution of 4.7% (1σ) for 5.3 MeV. This deterioration was thought to be due to the gain variation of the μ-PIC detection area.

3.3. Event reconstruction

Figure 5 shows a typical event display with the tracks and flash ADC waveform data for alpha-particle emission from ^{210}Po. The hit points were determined based on coincidence of anode and cathode detections. Figure 5 (c) shows the anode-cathode plane for the track. ~~The open circles are data~~ The open circles correspond to hits registered in data. The red solid line is a linear fit result. The dashed line represents the edge of the sample window. The solid blue point is the emission point of the alpha particle. The scheme of the determination of the emission point, or the track sense, is explained in Sec. 3.4. Figure 5 (a) and (d) show anode- and cathode-drift planes, respectively. The drift coordinate is converted from the timing and is set to zero base, which corresponds to the drift-plate position. Figure 5 (b) shows a flash ADC waveform.

The track angles were determined on the anode-cathode, anode-drift, and cathode-drift planes. These angles were determined with a common fitting algorithm. First, the weighted means of the hit points $(x_\mathrm{w}, y_\mathrm{w})$ were defined as

$$\begin{pmatrix} x_\mathrm{w} \\ y_\mathrm{w} \end{pmatrix} = \frac{1}{n} \sum_{j=0}^{n} \begin{pmatrix} x_j \\ y_j \end{pmatrix}, \quad (1)$$

where x_j and y_j are the measured hit points and n is ~~a~~the number of points. Next, the track was shifted and rotated through the angle θ as follows

$$\begin{pmatrix} x'_j \\ y'_j \end{pmatrix} = \begin{pmatrix} \cos\theta & -\sin\theta \\ \sin\theta & \cos\theta \end{pmatrix} \begin{pmatrix} x_j - x_\mathrm{w} \\ y_j - y_\mathrm{w} \end{pmatrix}. \quad (2)$$

Here x'_j and y'_j are the points after the ~~shift, and rotation and the angle~~ shift, the rotation angle θ

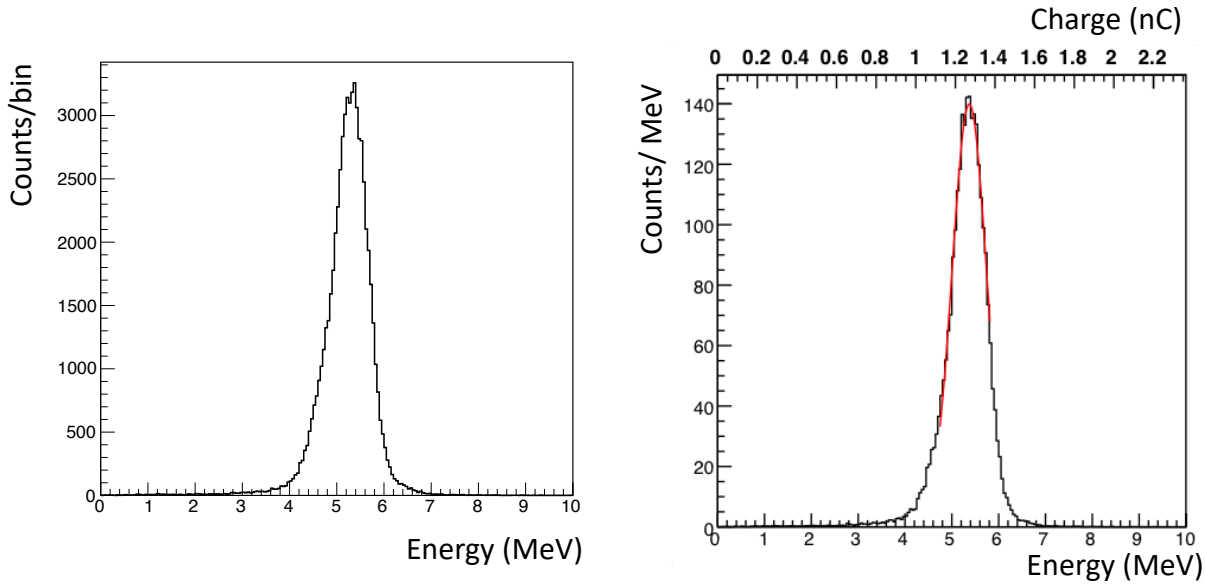

Fig. 4: (Left figure is old. Right figure is revised one.) Energy spectrum for alpha particles from ^{210}Po (5.3 MeV). Red line is a fit result with a Gaussian.

were determined to minimize the quantity f, which is defined as

$$f(\theta) = \sum y'^2_j, \tag{3}$$

where this formula means a sum of the square of the distance between the rotated point and the x axis. This method has the advantage to ~~determining~~determine the angle with no infinity pole at ~~$\theta = 90°$,~~ $\theta = 90°$ (i.e. parallel or perpendicular to the μ-PIC plane), in contrast with a ~~sample~~ linear fit.

3.4. Track-sense determination

Backgrounds in low radioactivity alpha-particle detectors are in general alpha particles from the radon (radon-α) and material in the detector (detector-α). The radon-α's are expected to be distributed uniformly in the gas volume with isotropic directions. The detector-α's are expected to have position and direction distributions specific to their sources. One of the main sources of the detector-α's ~~are the μ-PIC and the directions are mostly upward~~ is the μ-PIC so the directions of α's coming from this component are mostly upward-oriented. Since the direction of alpha particles from the sample are downward, these detector-α's and half of the radon-α's can be rejected by the cut of upward-direction events.

The deposit energy per unit path length, dE/dx of an alpha particle with an initial energy over a few MeV, has a peak before stopping (Bragg peak). The number of electrons ionized by the alpha particle in the gas is proportional to dE/dx, and dE/dx along the track profile is projected onto the time evolution in the signal due to the mechanism of the TPC. This time profile was recorded as the waveform and thus the track sense (i.e., whether the ~~tack~~track was upward or downward) can be determined from the waveform.

A parameter to determine the track sense is

$$F_{\mathrm{dwn}} = S_2/(S_1 + S_2), \tag{4}$$

where S_1 and S_2 are the time-integrated waveform before and after the peak. They are defined as

$$S_1 = \int_{t_0}^{t_p} v(t)dt, \tag{5}$$

$$S_2 = \int_{t_p}^{t_1} v(t)dt. \tag{6}$$

Here, $t_0 = 0$ μs, $t_1 = 1.5$ μs, and t_p are the start, stop, and peak time, respectively, for the waveform shown in Fig. 5 (b). The t_p is determined as a time when the voltage is the highest in region between t_0 and t_1. Figure 6 (a) shows typical F_{dwn} distribution with the alpha-particle source, where most of the events are expected to be downward-oriented. The F_{dwn} values of the downward events

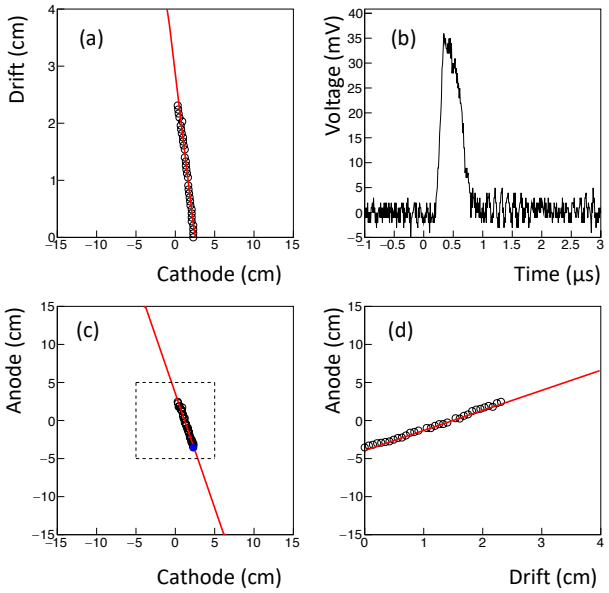

Fig. 5: Event display of an alpha particle from 210Po. (a) cathode-drift projection, (b) flash ADC waveform (c) cathode-anode projection, and (d) anode-drift projection are displayed. The drift coordinate is set to zero base corresponding to the drift plate position for the top of the track.

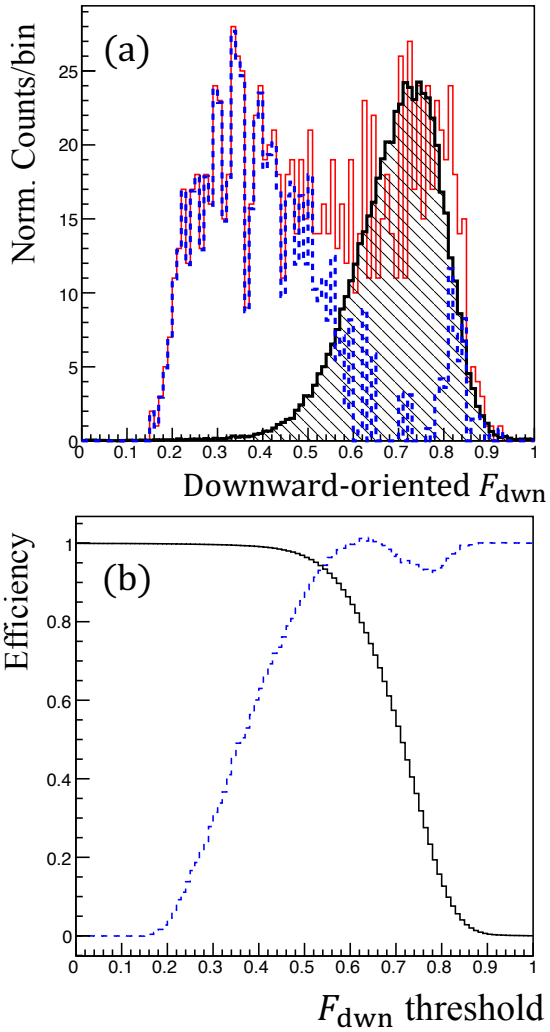

Fig. 6: (The figure (b) was added.) (a) Downward-oriented distribution for source-α (black shade), radon-α (red solid), and a histogram made by subtracting the radon-α spectrum from the source-α one(blue dashed). (b) Efficiency of downward-(black solid) and upward-oriented (blue dashed) events as a function of $F_{\rm dwn}$ threshold.

are distributed around 0.7, as shown by the black-shaded histograms. Conversely, radon-α's have an isotropic direction, ~~i.e., $F_{\rm dwn}$ has two peaks,~~ i.e., $F_{\rm dwn}$ has two components of upward- and downward-oriented, as shown by the red solid histogram, where the radon-α are background events in the sample test data, as explained later. The scale of the source-α was normalized to the radon-α peak of downward for clarity. Figure 6 (b) shows the efficiency related on $F_{\rm dwn}$ threshold for downward-(black solid) and upward-oriented (blue dashed). The selection efficiency of $F_{\rm dwn} > 0.5$ was estimated to be 0.964 ± 0.004 in the source-α spectrum while the radon background was reduced to half. The blue dashed histogram is a spectrum that subtracted the normalized source-α from the radon-α. The cut efficiency of the upward-oriented events ($F_{\rm dwn} \leq 0.5$) was estimated to be 0.85 ± 0.04. The energy dependence of $F_{\rm dwn}$ will be explained in Sec. 3.6.

3.5. Distribution of emission position

Since alpha particles are mainly emitted from the source, the top points of the alpha-particle tracks trace the shape of the radioactivity on the sample. Figures 7 (a) and 7 (b) show the anode–cathode projection distribution of the top and bottom of the alpha-particle tracks, respectively, where the top and bottom are defined as the zero and maximum drift coordinate, respectively, as shown in Fig. 5 (a) and 5 (d). The dashed line represents the edge of the drift-plate sample window. Comparing Fig. 7 (a) with Fig. 7 (b) clearly reveals the shape of the radioactivity.

The position resolution was evaluated along the four dashed lines in Fig. 7 (a). The number of events was projected onto the axis perpendicular to the lines and was fit with error functions as shown in Fig. 8. Figure 8 (a) and (b) represent the alpha-particle emission position projection to cathode and anode, respectively. The red lines are

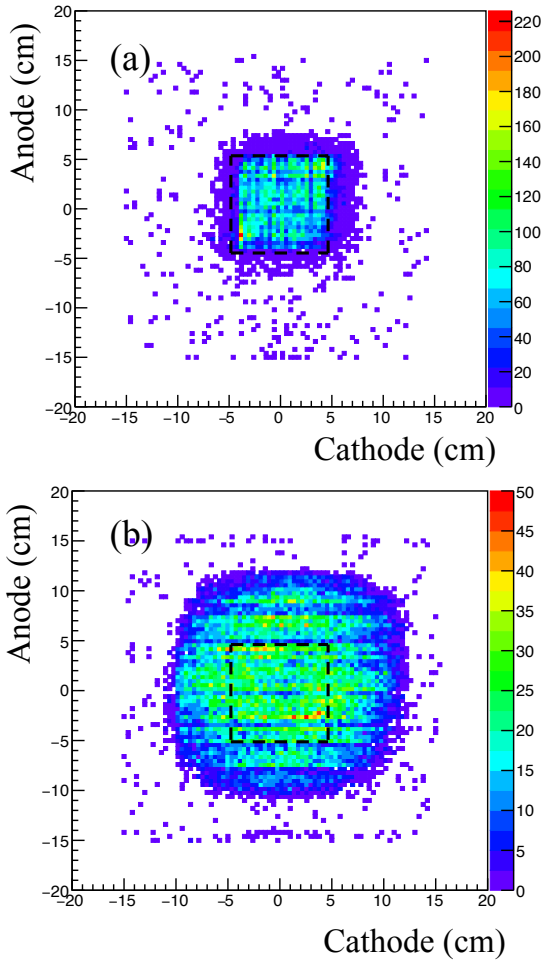

Fig. 7: Anode–cathode projection distributions of (a) top and (b) bottom of tracks for alpha particles emitted from the source. The dashed line is the edge of the sample window.

the fitting based on the error functions . As a result, the position resolution was determined to be 0.68 ± 0.14 cm (σ), where the error is a standard deviation in the four positions.

~~3.6. Efficiency of event selection~~

3.6. Detection and selection efficiency

To select good events for alpha particles from the sample, we use the following criteria: (C1) selection for events with good fitting tracks, (C2) cut for the upward-oriented events, and (C3) selection for events with emission points in the sample region.

For criterion C1, the good fit to track events was selected as $f_{\min}(\theta)/(n-1) < 0.02$ cm^2 for the anode-cathode, anode-drift, and cathode-drift

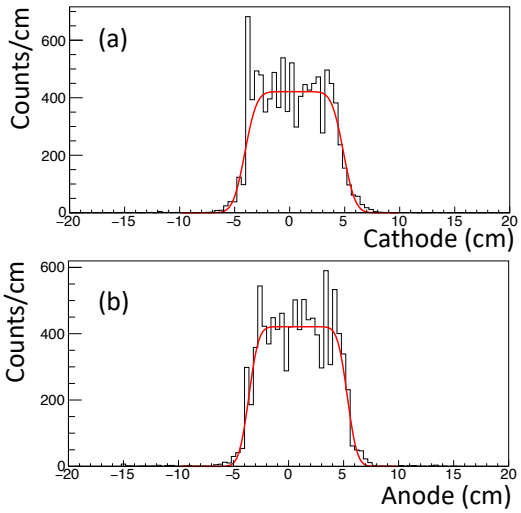

Fig. 8: (This figure was added.) Alpha-particle emission position projected to cathode (a) and anode (b). Red line represent fitting with error functions.

planes to remove events that had any noise and to remove candidates for electron tracks, where $f_{\min}(\theta)$ is a minimum of Eq. (3).

Criterion C2 rejects the upward-oriented tracks with > 3.5 MeV and $F_{\rm dwn} \leq 0.5$ because the determination efficiency depends on the energy. The upward- and downward-oriented tracks can be determined with 95% or more certainly at over 3.5 MeV. Note that this cut was applied for the events > 3.5 MeV, because the radon background, which was assumed to be the dominant background source, created the peak around 6 MeV and the contribution to the energy range below 3.5 MeV was limited.

~~For criterion C3, as shown in Fig. 7 (a), to reject the remained the radon and detector-α's, the selection region for alpha-particle emission point was set between -8.0 cm and 8.0 cm in both the anode and cathode coordinate.~~ For criterion C3, the source-α was selected within a region of ± 8 cm in both the anode and cathode, as shown in Fig. 7 (a). The rate of radon-α in the selected region was less than a few hundred time of source-α, ~~and thus the it was a negligible~~ considering it negligible.

The selection efficiency for C1, C2, and C3 containing the detection efficiency was calculated to be $(2.17 \pm 0.29) \times 10^{-1}$ counts/α (the ratio of the count rate to the α rate of the source), where the error represents the systematic error of C1 to C3 selections and ~~uncertainly~~uncertainty of the source

~~radioactivity and the statistic error is negligible~~ radioactivity, being the statistical error negligible.

3.7. Sample test and background estimate

3.7.1. Setup

A ~~5 × 5 cm^2~~ 5 cm × 5 cm piece of the standard μ-PIC whose α rate was known to be 0.28 ± 0.12 α/cm^2/hr in previous work [16] served as a sample and was inspected by using the detector. ~~The setup~~ A photograph of the sample position over the setup mesh is shown in Fig. 9. ~~The live time~~ The measurement live time was 75.85 hr.

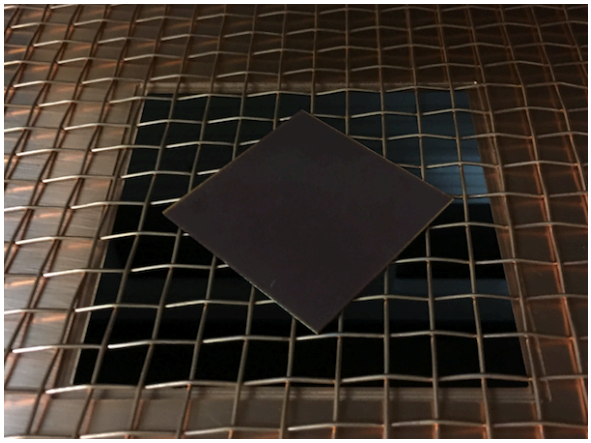

Fig. 9: ~~Fig. 8.~~ Setup for a ~~5 × 5 cm^2~~ 5 cm × 5 cm piece of the standard μ-PIC as sample.

3.7.2. Background in sample region

The α rate of the sample was estimated by subtracting the background rate. Considered background was mainly the radon-α. The detector measured both the α rates ~~on the region~~in the region of the sample and around the sample (outer region). The background rate could be determined from the α rate in the outer region. ~~The net α rate from the sample was thus evaluated by subtracting the background rate from the rate of the sample region. It was necessary to confirm that the background rates in both regions were consistent with each other.~~ Typically, the upward and downward radon-α rates are same. The sample-α has mainly downward-oriented. Thus, the background rate could be estimated by the upward rate in the sample region and independently cross-checked by the upward rate in the outer region.

We checked the upward-oriented ($F_{\mathrm{dwn}} \leq 0.5$) α rate in both regions because the alpha particles from a sample are typically emitted downward. Measured energy spectra are shown in Fig. 10. The red- and black-shaded histograms show the energy spectra inside and outside the sample region, respectively. These spectra are scaled by the selection efficiency. Both peaks are around 6 MeV and α rates are $(2.16^{+0.54}_{-0.35}) \times 10^{-2}$ (inside) and $(1.54^{+0.64}_{-0.40}) \times 10^{-2}$ α/cm^2/hr (outside). Therefore, the background condition inside the sample region ~~is consistent~~ is compatible at less than 1σ with the background condition outside the sample region. The alpha-particle energy spectrum is interpreted as the radon peaks at 5.5 MeV (^{222}Rn), 6.0 MeV (^{218}Po), and 7.7 MeV (^{214}Po).

The downward-oriented ($F_{\mathrm{dwn}} > 0.5$) α rate outside the sample is $(1.58^{+0.29}_{-0.26}) \times 10^{-2}$ α/cm^2/hr, as shown in the black-shaded spectrum of Fig. 12. In this work, the background rate was improved by one order of magnitude in comparison with that of our previous work [16]. The background reduction is attributed to the track-sense determination to reject upward-oriented alpha (for > 3.5 MeV) and the replacement of the low-α μ-PIC (for ≤ 3.5 MeV). In the energy region between 2.0 and 4.0 MeV, where most radon background is suppressed, the background rate is $(9.6^{+7.9}_{-5.6}) \times 10^{-4}$ α/cm^2/hr.

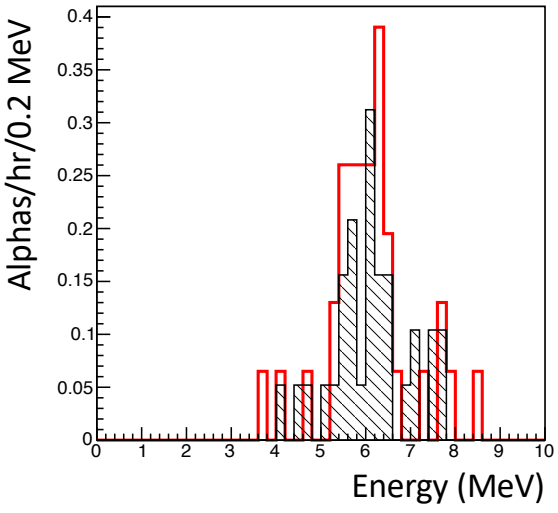

Fig. 10: ~~Fig. 9.~~ ~~Downward-oriented~~ Upward-oriented alpha-particle energy spectra inside (red) and outside (black shade) the sample region.

3.7.3. α rate of sample

Figure 11 shows the distribution of the top of the tracks for the sample, where the candidates are selected by the criteria C1 and C2. ~~The regions ① and ② are sample and background regions, respectively.~~ The regions ① and ② are defined as sample and background regions, respectively. The sample region corresponds to the sample window. The sample region is the inside of ±5 cm of anode and cathode. The background region is the outside of the sample region and the inside of ±7.5 cm of anode and cathode. Figure 12 shows the energy spectra of downward-oriented alpha particles in the sample (red) and the background region (black shaded). The α rate of the sample was calculated to be $(3.57^{+0.35}_{-0.33}) \times 10^{-1}$ $\alpha/\mathrm{cm}^2/\mathrm{hr}$ (> 2.0 MeV) by subtracting the background rate.

~~Assuming the alpha spectrum is constituted only from ^{232}Th or ^{238}U, the impurity is estimated to be 6.0 ± 1.4 or 3.0 ± 0.7 ppm, respectively.~~ Here, the impurity of ^{232}Th and ^{238}U is estimated by comparing with a prediction of α rate spectrum in the simulation, where it mentions that the isotope in the material is assumed as only ^{232}Th or ^{238}U because of the continuous α rate spectrum. In the fit region between 2 and 10 MeV, the impurity of ^{232}Th or ^{238}U is estimated to be 6.0 ± 1.4 or 3.0 ± 0.7 ppm, respectively. The impurities of ^{232}Th and ^{238}U are measured to be 5.84 ± 0.03 and 2.31 ± 0.02 ppm, respectively, by using the HPGe detector with the measuring time of 308 hr. Although the error is huge because of the continuous energy spectrum, it is consistent with the prediction of prior measurement. In this sample test, it was demonstrated to observe the background alphas at the same time.

4. Discussion

We begin by discussing the sensitivity for the energy between 2 and 9 MeV based on long-term measurements. In this energy range, the background is dominated by the radon-α's with $\sim (1.58^{+0.29}_{-0.26}) \times 10^{-2}$ $\alpha/\mathrm{cm}^2/\mathrm{hr}$. The statistical error (σ) is expected to scale with the inverse of the square root of the measurement time (t) given as $\sigma \propto 1/\sqrt{t}$. In this work, the live time was only three days, and the statistical error was $\sigma \sim 3 \times 10^{-3}$ $\alpha/\mathrm{cm}^2/\mathrm{hr}$. With a measurement time of one month, the error of ~~radon-a~~sample-α's was estimated to be $\sigma \sim 1 \times 10^{-3}$ $\alpha/\mathrm{cm}^2/\mathrm{hr}$. When the α rate ($\sigma \sim 1 \times 10^{-3}$ $\alpha/\mathrm{cm}^2/\mathrm{hr}$) as the same

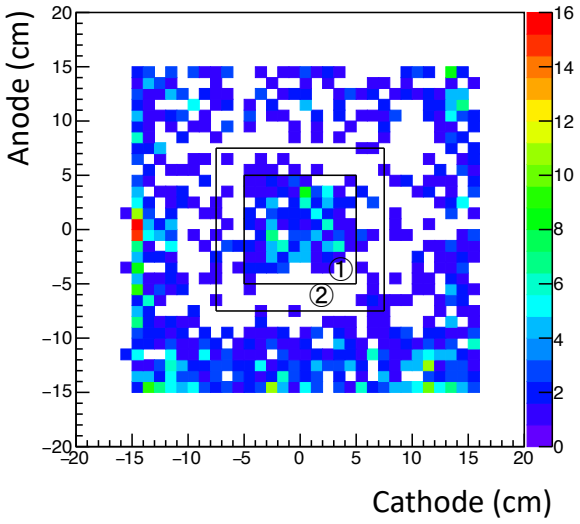

Fig. 11: ~~Fig. 10.~~ Distribution of the top of downward-oriented alpha-particle track. The regions ① and ② are the sample and background regions, respectively.

of the radon-α's ($\sigma \sim 1 \times 10^{-3}$ $\alpha/\mathrm{cm}^2/\mathrm{hr}$) was observed, the sum of squares of these σs for the sample and radon-α's would be expected to be a few 10^{-3} $\alpha/\mathrm{cm}^2/\mathrm{hr}$ as the measurement limit by subtraction with these α rates.

The edges region (anode $\sim \pm 15$ cm or cathode $\sim \pm 15$ cm) has a high rate of background, as shown in Fig. 11. These events have an energy and path-length dependence similar to that of the alpha particles. The alpha particles were mainly oriented upward and were emitted from outside the detection area, limited by the μ-PIC. As an impurity candidate, a piece of the printed circuit board (PCB) was inspected and the α rate was $(1.16 \pm 0.06) \times 10^{-1}$ $\alpha/\mathrm{cm}^2/\mathrm{hr}$. Although the alpha-particle events could be rejected by the fiducial region cut, these impurities could be the radon sources (see Fig. 13). Therefore, as a next improvement, a material with less radiative impurities should be used for the PCB.

The goal for detector sensitivity is less than 10^{-4} $\alpha/\mathrm{cm}^2/\mathrm{hr}$, which corresponds to measuring radioactive impurities at the ppb level. Here, this level was estimated as an assumption of ^{238}U or ^{232}Th in 1-mm-thick copper plate. We can potentially improve the background rate by using the cooled charcoal to suppress radon gas and using a material with less impurities such as polytetrafluoroethylene, polyimide, and polyetheretherketone without glass fibers. A recent study reported that

	This work	HPGe detector
Sample volume (cm)	$(5 \times 5) \times 0.098$	$(5 \times 5) \times 2.47$
Sample weight (g)	6.8	169.5
Measureing time (hr)	75.85	308
Net α rate (α/cm^2/hr))	$(3.57^{+0.35}_{-0.33}) \times 10^{-1}$	—
^{232}Th impurities (ppm)	6.0 ± 1.4	5.84 ± 0.03
^{238}U impurities (ppm)	3.0 ± 0.7	2.31 ± 0.02

Table 1: (The table was added.) Comparison of Screening result with this work and HPGe detector.

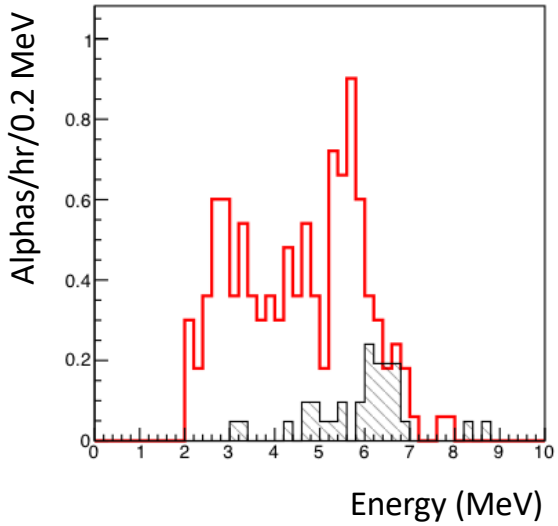

Fig. 12: ~~Fig. 11.~~ Downward-oriented alpha-particle energy spectra in sample region (red) and background region (black shade).

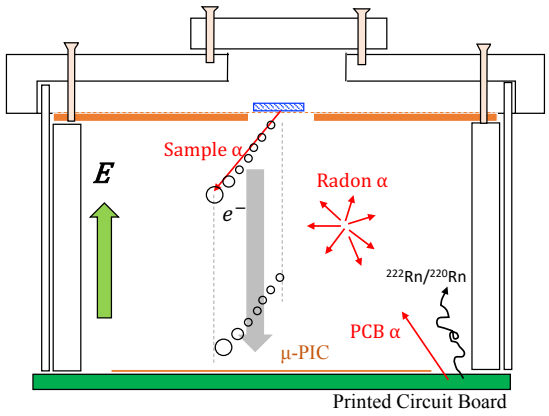

Fig. 13: ~~Fig. 12.~~ Schematic cross section of background alpha particles in detector setup.

a cooled charcoal could suppress the radon by 99% in the argon gas [20]. A recent NEWAGE detector suppresses the radon to 1/50 by using cooled charcoal [5]. With these improvements, the detector would ~~achieved~~achieve to the goal of performance.

5. Conclusion

We developed a new alpha-particle imaging detector based on the gaseous micro-TPC. The measured energy resolution is 6.7% (σ) for 5.3 MeV alpha particles. The measured position resolution is 0.68 ± 0.14 cm. Based on a waveform analysis, the downward-oriented events' selection efficiency is 0.964 ± 0.004 and the cut efficiency of the upward-oriented events is 0.85 ± 0.04 at > 3.5 MeV. Also, a piece of the standard μ-PIC was measured as a sample, and the result is consistent ~~with the one by another measurement~~ with the one obtained by a measurement done with a HPGe detector. A measurement of the alpha particles from a sample and background was also established at the same time. A background rate near the radon-α ($(1.58^{+0.51}_{-0.42}) \times 10^{-2}$ α/cm^2/hr) was achieved.

Acknowledgments

This work was supported by a Grant-in-Aid for Scientific Research on Innovative Areas, 26104004 and 26104008, from the Japan Society for the Promotion of Science in Japan. This work was supported by the joint research program of the Institute for Cosmic Ray Research (ICRR), the University of Tokyo. We thank Dr. Y. Nakano of the ICRR, University of Tokyo, Japan for providing us with a helium-gas leak detector.

References

[1] R Bernabei, et al., J. Phys. Conf. Ser. **1056** (2018) 012005.
[2] XENON Collaboration, Eur. Phys. J. **77** 881 (2017).
[3] D. S. Akerib, et al., Phys. Rev. Lett. **118** 021303 (2017).

[4] T. Tanimori, et al., Phys. Lett. B **578** (2004) 241.
[5] K. Nakamura, et al., Prog. Theo. Exp. Phys. (2015) 043F01.
[6] The GERDA Collaboration, Nature **544** (2017) 47.
[7] ~~K. Asakura, et al., Nucl. Phys. A **946** (2016) 171.~~
A. Gando, et al., Phys. Rev. Lett. **117** 082503 (2016).
[8] D. S. Leonard, et al., Nucl. Instr. Meth. A **871** (2017) 169.
[9] N. Abgrall, et al., Nucl. Instr. Meth. A **828** (2016) 22.
[10] R. Arnold, et al., Eur. Phys. J. C **78** (2018) 821.
[11] R. Arnold, et al., PRL **119**, 041801 (2017).
[12] A. S. Barabash, et al., JINST **12** (2017) P06002.
[13] K. Abe, et al., Nucl. Instr. Meth. A **884** (2018) 157.
[14] K. Miuchi, et al., Phys. Lett. B **686** (2010).
[15] K. Miuchi, et al., Phys. Lett. B **654** (2007) 58.
[16] T. Hashimoto, et al., AIP Conf. Proc. **1921**, 070001 (2018).
[17] T. Hashimoto, et al., in preparation.
[18] R. Orito, et al., IEEE Trans. Nucl. Scie. **51**, 4 (2004) 1337.
[19] H. Kubo, et al., Nucl. Instr. Meth. A **513** (2003) 93.
[20] M. Ikeda, et al., Radioisotopes, **59**, (2010) 29.